

Electronic Supplementary Information

Cu(II)-catalyzed enantioselective oxygen atom transfer from oxaziridine to oxindole derivatives with chiral phenanthroline

Yuki Naganawa,* Tomotaka Aoyama, and Hisao Nishiyama*

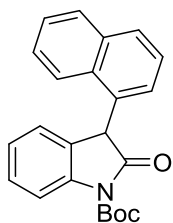
Department of Applied Chemistry, Graduate School of Engineering, Nagoya University,
Chikusa, Nagoya 464-8603, Japan

General Information. Infrared (IR) spectra were recorded on a JASCO FT/IR-230 spectrometer. ¹H NMR spectra were measured at 25 °C on a Varian Mercury 300 (300 MHz) spectrometer. Data were reported as follows: chemical shifts in ppm from tetramethylsilane as an internal standard, integration, multiplicity (s = singlet, d = doublet, t = triplet, q = quartet, dd = double-doublet, ddd = double-double-doublet, dt = double-triplet, m = multiplet, br = broad, and app = apparent), coupling constants (Hz), and assignment. ¹³C NMR spectra were measured at 25 °C on a Varian Mercury 300 (75 MHz) spectrometer with complete proton decoupling. Chemical shifts were reported in ppm from the residual solvent as an internal standard. High performance liquid chromatography (HPLC) was performed carried out on a JASCO GULLIVER 1500 series using 4.6 mm x 25 cm Daicel Chiral Columns. High-resolution mass spectra (HRMS) were performed on a double-focusing magnetic sector mass spectrometer JEOL JMS-700. For thin layer chromatography (TLC) analysis throughout this work, TLC Silica gel 60 F₂₅₄ were used. The products were purified by flash column chromatography on silica gel 60 N (Kanto, 60-210 μm).

In experiments requiring dry solvent, CH₂Cl₂, diethyl ether and isopropyl alcohol were purchased from Wako Pure Chemical Industries as “Dehydrated”. CPME was purchased from Sigma-Aldrich as “Dehydrated”. Toluene and THF were purchased from Kanto Chemical as “Dehydrated” and further purified by passing through neutral alumina under nitrogen atmosphere. BinThro ligands (*S*)-**1** were prepared according to our previous report.^{S1} Oxindole derivatives **2**^{S2} and Davis’ oxaziridine **3**^{S3} were synthesized according to the literature, respectively.

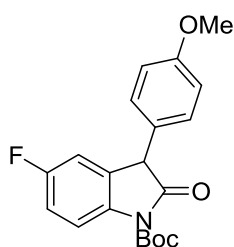
•Spectroscopic data and NMR spectra for new oxindole derivatives (2)

***N*-*t*-Butoxycarbonyl-3-(1-naphthyl)-2-oxindole (2g).**



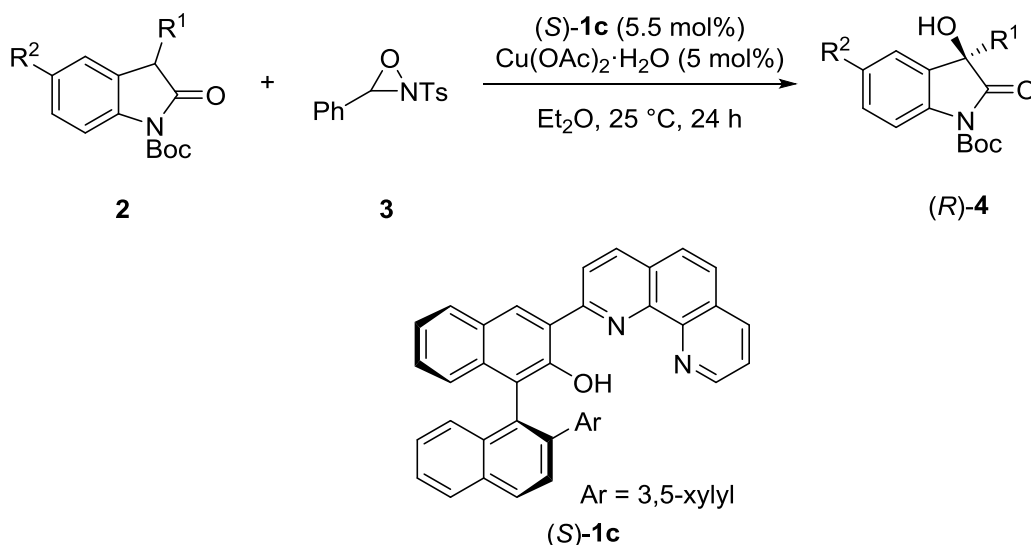
IR (KBr): 3050, 2976, 1784, 1598, 1511, 1480, 1394, 1352, 1299, 1143, 1092, 1048, 1023 cm^{-1} ; ^1H NMR (300 MHz, CDCl_3): δ (ppm) = 8.33 (br, 1H), 8.00 (d, $J = 8.1$ Hz, 1H), 7.90 (d, $J = 8.7$ Hz, 1H), 7.83 (d, $J = 8.4$ Hz, 1H), 7.53 (br, 2H), 7.38 (t, $J = 8.4$ Hz, 2H), 7.13 (d, $J = 6.6$ Hz, 3H), 5.64 (br, 1H), 1.65 (s, 9H); ^{13}C NMR (75 MHz, CDCl_3): δ (ppm) = 173.4, 149.2, 134.0, 128.7, 128.4, 127.9, 126.5, 125.8, 125.2, 124.5, 123.7, 115.0, 84.4, 48.1, 28.2 (Six peaks were overlapped.); HRMS (FAB) Calcd for $\text{C}_{23}\text{H}_{21}\text{NO}_3$ ($[\text{M}]^+$) 359.1521. Found 359.1515.

***N*-*t*-Butoxycarbonyl-5-fluoro-3-(*p*-methoxyphenyl)-2-oxindole (2n).**



IR (KBr): 2982, 1774, 1717, 1608, 1510, 1485, 1371, 1346, 1296, 1249, 1146, 1093, 1036 cm^{-1} ; ^1H NMR (300 MHz, CDCl_3): δ (ppm) = 7.89-7.93 (m, 1H), 7.05-7.11 (m, 3H), 6.87-6.90 (m, 3H), 4.66 (s, 1H), 3.80 (s, 3H), 1.63 (s, 9H); ^{13}C NMR (75 MHz, CDCl_3): δ (ppm) = 173.4, 159.6 (d, $J = 242$ Hz), 159.1, 149.1, 136.1 (d, $J = 2.3$ Hz), 129.3 (d, $J = 9.1$ Hz), 129.2, 127.4, 116.2 (d, $J = 7.4$ Hz), 115.0 (d, $J = 22.2$ Hz), 114.3, 112.3 (d, $J = 24.0$ Hz), 84.5, 55.4, 51.9 (d, $J = 1.7$ Hz), 28.2; HRMS (FAB) Calcd for $\text{C}_{20}\text{H}_{20}\text{FNO}_4$ ($[\text{M}]^+$) 357.1376. Found 357.1376.

•General procedure for enantioselective C-H oxidation of oxindoles (2).



To a mixture of (*S*)-**1c** (3.0 mg, 5.5 μ mol) and $\text{Cu}(\text{OAc})_2 \cdot \text{H}_2\text{O}$ (1.0 mg, 5.0 μ mol) in schlenk tube under Ar atmosphere, dry diethyl ether (1 mL) were added at 25 $^\circ\text{C}$. After stirring for 1 h at 25 $^\circ\text{C}$, oxindole **2** (0.1 mmol) was added portion-wise to the mixture. After stirring another 5 min, Davis' oxaziridine **3** (33.0 mg, 0.12 mmol) was added portion-wise to the mixture and stirred for 24 h at the same temperature. The catalyst was removed by passing through short column chromatography on silica gel (eluting chloroform) and the solvent was evaporated. The residue was purified by column chromatography (eluting hexane/EtOAc) to give the desired product (*R*)-**4**.

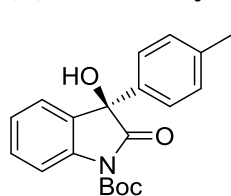
(*R*)-*N*-*t*-Butoxycarbonyl-3-hydroxy-3-phenyl-2-oxindole (4a).



^1H NMR (300 MHz, CDCl_3): δ (ppm) = 7.94 (d, J = 7.8 Hz, 1H), 7.17-7.49 (m, 8H), 3.37 (s, 1H), 1.64 (s, 9H). The detailed spectral data has been reported in the literature.^{S2}

The enantiomeric purity of the product was determined by HPLC analysis (Daicel CHIRALCEL AD-H, hexane/*i*PrOH = 95/5, flow rate = 0.5 mL/min, retention time; 26.1 min (*R*) and 56.5 min (*S*)). [e.r. = 97.5/2.5][e.e. = 95.0%]

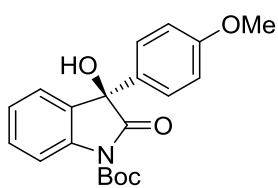
(*R*)-*N*-*t*-Butoxycarbonyl-3-hydroxy-3-(4-methylphenyl)-2-oxindole (4b).



^1H NMR (300 MHz, CDCl_3): δ (ppm) = 7.96 (d, J = 8.1 Hz, 1H), 7.18-7.43 (m, 7H), 3.37 (s, 1H), 2.36 (s, 3H), 1.67 (s, 9H). The detailed spectral data has been reported in the literature.^{S2}

The enantiomeric purity of the product was determined by HPLC analysis (Daicel CHIRALCEL AD-H, hexane/*i*PrOH = 95/5, flow rate = 0.5 mL/min, retention time; 15.1 min (*R*) and 28.3 min (*S*)). [e.r. = 98.0/2.0][e.e. = 96.0%]

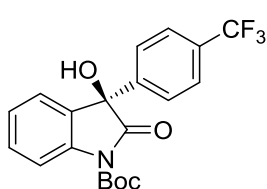
(R)-N-t-Butoxycarbonyl-3-hydroxy-3-(4-methoxyphenyl)-2-oxindole (4c).



IR (KBr): 3444, 2979, 1779, 1732, 1609, 1510, 1467, 1370, 1344, 1289, 1253, 1149, 1102, 1034 cm^{-1} ; ^1H NMR (300 MHz, CDCl_3): δ (ppm) = 7.92 (d, J = 8.1 Hz, 1H), 7.20-7.42 (m, 5H), 6.85 (dd, J = 2.1 Hz, 6.9 Hz, 2H), 3.78 (s, 3H), 3.36 (s, 1H), 1.62 (s, 9H); ^{13}C NMR (75 MHz, CDCl_3): δ (ppm) = 175.6, 159.5, 148.8, 139.3, 131.5, 129.9, 128.0, 126.9, 125.0, 124.8, 115.2, 113.8, 84.8, 77.2, 55.4, 28.2; $[\alpha]_{\text{D}}^{26}$ = +17.1 (c = 0.98, CHCl_3); HRMS (FAB) Calcd for $\text{C}_{20}\text{H}_{21}\text{NO}_5$ ($[\text{M}+\text{Na}]^+$) 378.1317. Found 378.1317.

The enantiomeric purity of the product was determined by HPLC analysis (Daicel CHIRALCEL AD-H, hexane/*i*PrOH = 95/5, flow rate = 0.8 mL/min, retention time; 30.5 min (*R*) and 53.8 min (*S*)). [e.r. = 96.5/3.5][e.e. = 93.0%]

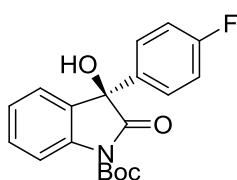
(R)-N-t-Butoxycarbonyl-3-hydroxy-3-(4-trifluoromethylphenyl)-2-oxindole (4d).



IR (KBr): 3821, 3448, 2983, 1793, 1737, 1609, 1468, 1413, 1372, 1327, 1253, 1150, 1069, 1018 cm^{-1} ; ^1H NMR (300 MHz, CDCl_3): δ (ppm) = 7.96 (d, J = 8.4 Hz, 1H), 7.43-7.61 (m, 5H), 7.22-7.26 (m, 2H), 3.44 (s, 1H), 1.64 (s, 9H); ^{13}C NMR (75 MHz, CDCl_3): δ (ppm) = 174.8, 148.6, 143.3, 139.4, 130.5 (q, J = 32.5 Hz), 130.4, 129.4, 125.9, 125.4 (q, J = 4.0 Hz), 125.4, 124.8, 123.6 (q, J = 270 Hz), 115.5, 85.2, 77.2, 28.2; $[\alpha]_{\text{D}}^{26}$ = +19.1 (c = 0.63, CHCl_3); HRMS (FAB) Calcd for $\text{C}_{20}\text{H}_{18}\text{FNO}_4$ ($[\text{M}+\text{Na}]^+$) 416.1086. Found 416.1103.

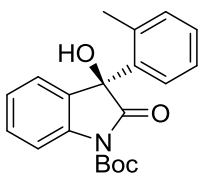
The enantiomeric purity of the product was determined by HPLC analysis (Daicel CHIRALCEL AD-H, hexane/*i*PrOH = 95/5, flow rate = 1.0 mL/min, retention time; 9.4 min (*R*) and 14.6 min (*S*)). [e.r. = 97.4/2.6][e.e. = 94.8%]

(R)-N-t-Butoxycarbonyl-3-hydroxy-3-(4-fluorophenyl)-2-oxindole (4e).



^1H NMR (300 MHz, CDCl_3): δ (ppm) = 7.94 (d, J = 8.4 Hz, 1H), 7.22-7.44 (m, 5H), 7.20 (dt, J = 15 Hz, 0.9 Hz, 1H), 3.34 (s, 1H), 1.63 (s, 9H). The detailed spectral data has been reported in the literature.^{S2}
The enantiomeric purity of the product was determined by HPLC analysis (Daicel CHIRALCEL AD-H, hexane/*i*PrOH = 95/5, flow rate = 1.0 mL/min, retention time; 13.8 min (*R*) and 24.1 min (*S*)). [e.r. = 97.5/2.5][e.e. = 95.0%]

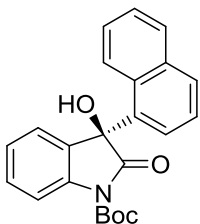
(R)-N-t-Butoxycarbonyl-3-hydroxy-3-(2-methylphenyl)-2-oxindole (4f).



IR (KBr): 3865, 3803, 3751, 3446, 3059, 2980, 2931, 1730, 1608, 1480, 1292, 1149, 1094, 1036 cm^{-1} ; ^1H NMR (300 MHz, CDCl_3): δ (ppm) = 7.90-7.95 (m, 2H), 7.22-7.42 (m, 4H), 7.05-7.16 (m, 3H), 3.18 (s, 1H), 1.88 (s, 3H), 1.67 (s, 9H); ^{13}C NMR (75 MHz, CDCl_3): δ (ppm) = 175.0, 148.8, 139.9, 137.3, 134.3, 131.4, 130.1, 128.7, 128.4, 125.9, 125.6, 125.1, 124.7, 115.2, 84.8, 77.3, 28.2, 19.8; $[\alpha]_{\text{D}}^{26} = +86.5$ (c = 0.97, CHCl_3); HRMS (FAB) Calcd for $\text{C}_{20}\text{H}_{21}\text{NO}_4$ ($[\text{M}+\text{H}]^+$) 340.1549. Found 340.1560.

The enantiomeric purity of the product was determined by HPLC analysis (Daicel CHIRALCEL AD-H, hexane/*i*PrOH = 95/5, flow rate = 0.5 mL/min, retention time; 31.0 min (*R*) and 103.6 min (*S*)). [e.r. = 90.0/10.0][e.e. = 80.0%]

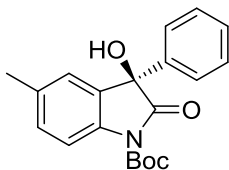
(R)-N-t-Butoxycarbonyl-3-hydroxy-3-(1-naphthyl)-2-oxindole (4g).



IR (KBr): 3444, 2980, 1733, 1607, 1511, 1479, 1287, 1155, 1101, 1002, cm^{-1} ; ^1H NMR (300 MHz, CDCl_3): δ (ppm) = 8.03 (d, $J = 8.1$ Hz, 1H), 7.91 (d, $J = 6.9$ Hz, 1H), 7.84-7.90 (m, 2H), 7.70 (d, 1H), 7.33-7.53 (m, 5H), 7.18-7.20 (m, 1H), 7.06-7.12 (m, 1H), 3.41 (s, 1H), 1.68 (s, 9H); ^{13}C NMR (75 MHz, CDCl_3): δ (ppm) = 175.0, 149.0, 139.4, 134.3, 134.1, 130.3, 130.1, 129.8, 129.7, 128.9, 126.4, 125.4, 125.1, 124.8, 124.71, 124.68, 124.0, 115.6, 84.9, 78.3, 28.2; $[\alpha]_{\text{D}}^{26} = +93.0$ (c = 1.0, CHCl_3); HRMS (FAB) Calcd for $\text{C}_{23}\text{H}_{21}\text{NO}_4$ ($[\text{M}]^+$) 375.1471. Found 375.1466.

The enantiomeric purity of the product was determined by HPLC analysis (Daicel CHIRALCEL AD-H, hexane/*i*PrOH = 95/5, flow rate = 0.5 mL/min, retention time; 40.0 min (*R*) and 98.0 min (*S*)). [e.r. = 83.5/16.5][e.e. = 67.0%]

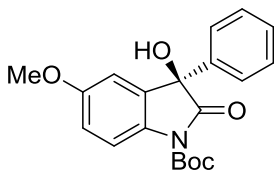
(R)-N-t-Butoxycarbonyl-3-hydroxy-5-methyl-3-phenyl-2-oxindole (4h).



^1H NMR (300 MHz, CDCl_3): δ (ppm) = 7.81 (d, $J = 8.4$ Hz, 1H), 7.30-7.35 (m, 5H), 7.11-7.21 (m, 2H), 7.11 (d, $J = 0.6$ Hz, 1H) 3.26 (s, 1H), 2.33 (s, 3H) 1.64 (s, 9H); The detailed spectral data has been reported in the literature.^{S2}

The enantiomeric purity of the product was determined by HPLC analysis (Daicel CHIRALCEL AD-H, hexane/*i*PrOH = 95/5, flow rate = 0.8 mL/min, retention time; 18.6 min (*R*) and 32.0 min (*S*)). [e.r. = 97.8/2.2][e.e. = 95.6%]

(R)-N-t-Butoxycarbonyl-3-hydroxy-5-methoxy-3-phenyl-2-oxindole (4i).

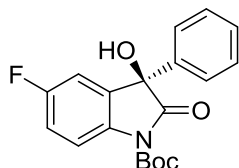


^1H NMR (300 MHz, CDCl_3): δ (ppm) = 7.86 (d, $J = 9.0$ Hz, 1H), 7.26-7.36 (m, 5H), 6.93 (dd, $J = 9.0$ Hz, 2.4 Hz, 1H), 6.85 (d, 2.7 Hz, 1H), 3.77 (s, 3H), 3.31 (br, 1H), 1.63 (s, 9H).; $[\alpha]_{\text{D}}^{25} = +31.6$ (c

= 1.0, CHCl₃). The detailed spectral data has been reported in the literature.^{S2}

The enantiomeric purity of the product was determined by HPLC analysis (Daicel CHIRALCEL AD-H, hexane/*i*PrOH = 95/5, flow rate = 0.8 mL/min, retention time; 30.0 min (*R*) and 54.0 min (*S*)). [e.r. = 96.9/3.1][e.e. = 93.8%]

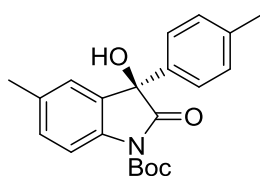
(*R*)-*N*-*t*-Butoxycarbonyl-3-hydroxy-5-fluoro-3-phenyl-2-oxindole (4j).



IR (KBr): 3429, 2927, 1789, 1732, 1610, 1511, 1485, 1371, 1341, 1297, 1252, 1149, 1108, 1034, cm⁻¹; ¹H NMR (300 MHz, CDCl₃): δ (ppm) = 7.94 (dd, *J* = 4.8 Hz, 9.0 Hz, 1H), 7.33 (m, 5H), 7.01-7.13 (m, 2H), 3.35 (s, 1H), 1.64 (s, 9H); ¹³C NMR (75 MHz, CDCl₃): δ (ppm) = 175.2, 159.9 (d, *J* = 243 Hz), 148.6, 139.0, 135.2 (d, *J* = 2.3 Hz), 131.6 (d, *J* = 8.0 Hz), 128.6, 125.9, 125.1, 116.8 (d, *J* = 4.0 Hz), 116.6 (d, *J* = 19.4 Hz), 112.3 (d, *J* = 2.4 Hz), 85.1, 77.6 (d, *J* = 1.7 Hz), 28.2; [α]_D²³ = +69.6 (c = 0.71, CHCl₃). HRMS (FAB) Calcd for C₁₉H₁₈FNO₄ ([M+Na]⁺) 366.1118. Found 366.1122.

The enantiomeric purity of the product was determined by HPLC analysis (Daicel CHIRALCEL AD-H, hexane/*i*PrOH = 95/5, flow rate = 0.8 mL/min, retention time; 14.5 min (*R*) and 25.5 min (*S*)). [e.r. = 97.3/2.7][e.e. = 94.6%]

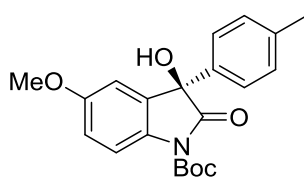
(*R*)-*N*-*t*-Butoxycarbonyl-3-hydroxy-5-methyl-3-(4-methylphenyl)-2-oxindole (4k).



¹H NMR (300 MHz, CDCl₃): δ (ppm) = 7.80 (d, *J* = 8.4 Hz, 1H), 7.12-7.23 (m, 6H), 3.25 (s, 1H), 2.33 (s, 3H), 2.32 (s, 3H), 1.63 (s, 9H). The detailed spectral data has been reported in the literature.^{S2}

The enantiomeric purity of the product was determined by HPLC analysis (Daicel CHIRALCEL AD-H, hexane/*i*PrOH = 95/5, flow rate = 1.0 mL/min, retention time; 16.5 min (*R*) and 27.0 min (*S*)). [e.r. = 97.3/2.7][e.e. = 94.6%]

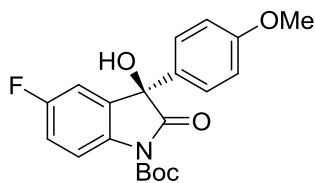
(*R*)-*N*-*t*-Butoxycarbonyl-3-hydroxy-5-methoxy-3-(4-methylphenyl)-2-oxindole (4l).



IR (KBr): 3444, 2979, 1779, 1733, 1609, 1510, 1467, 1370, 1344, 1289, 1252, 1149, 1102, 1034, cm⁻¹; ¹H NMR (300 MHz, CDCl₃): δ (ppm) = 7.86 (d, *J* = 9.0 Hz, 1H), 7.23-7.26 (m, 2H), 7.70 (d, *J* = 8.4 Hz, 2H), 6.92 (dd, *J* = 2.7 Hz, 8.7 Hz 1H), 6.86 (d, *J* = 2.7 Hz 1H), 3.77 (s, 3H), 3.18 (s, 1H), 2.33 (s, 3H), 1.63 (s, 9H); ¹³C NMR (75 MHz, CDCl₃): δ (ppm) = 175.6, 157.0, 148.8, 138.2, 136.5, 132.6, 131.1, 129.1, 125.2, 116.3, 115.4, 110.1, 84.5, 77.8, 55.7, 28.2, 21.3; [α]_D²⁵ = -1.0 (c = 1.0, CHCl₃); HRMS (FAB) Calcd for C₂₁H₂₃NO₅ ([M+Na]⁺) 392.1474. Found 392.1479.

The enantiomeric purity of the product was determined by HPLC analysis (Daicel CHIRALCEL AD-H, hexane/*i*PrOH = 95/5, flow rate = 1.0 mL/min, retention time; 27.2 min (*R*) and 50.7 min (*S*)). [e.r. = 97.9/2.1][e.e. = 95.8%]

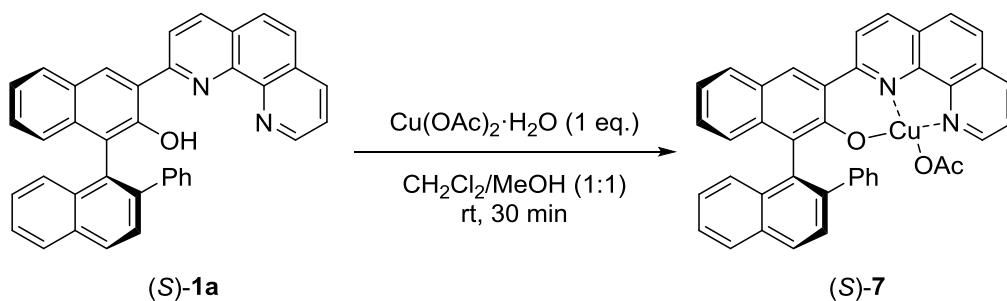
(*R*)-*N*-*t*-Butoxycarbonyl-3-hydroxy-5-fluoro-3-(4-methoxyphenyl)-2-oxindole (4m).



IR (KBr): 3821, 3448, 2983, 1793, 1737, 1609, 1468, 1413, 1372, 1327, 1254, 1150, 1069, 1018 cm^{-1} ; ^1H NMR (300 MHz, CDCl_3): δ (ppm) = 7.90-7.95 (m, 1H), 7.28 (d, $J = 2.1$ Hz, 1H), 7.03-7.13 (m, 2H), 6.87 (dd, $J = 6.9$ Hz, 9.3 Hz, 2H), 3.79 (s, 3H), 3.33 (s, 1H), 1.63 (s, 9H); ^{13}C NMR (75 MHz, CDCl_3): δ (ppm) = 175.3, 159.9 (d, $J = 243$ Hz), 159.6, 148.7, 135.2, 131.6 (d, $J = 8.0$ Hz), 131.0, 126.7, 116.8 (d, $J = 7.4$ Hz), 116.4, 114.0, 112.3 (d, $J = 24.0$ Hz), 85.0, 77.2 (d, $J = 5.1$ Hz), 55.4, 28.2; $[\alpha]_{\text{D}}^{27} = +21.0$ ($c = 0.84$, CHCl_3); HRMS (FAB) Calcd for $\text{C}_{20}\text{H}_{20}\text{FNO}_5$ ($[\text{M}+\text{Na}]^+$) 396.1223. Found 396.1222.

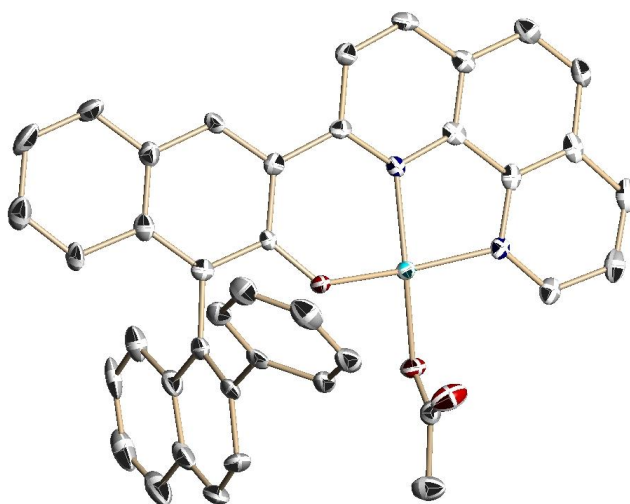
The enantiomeric purity of the product was determined by HPLC analysis (Daicel CHIRALCEL AD-H, hexane/*i*PrOH = 95/5, flow rate = 0.5 mL/min, retention time; 25.1 min (*R*) and 41.5 min (*S*)). [e.r. = 97.24/2.76][e.e. = 94.48%]

•General procedure for the preparation of Cu complex (S)-7.



A yellow solution of BinThro (S)-1a (52.4 mg, 0.1 mmol) in CH₂Cl₂ (5 mL) was added to a pale blue solution of Cu(OAc)₂·H₂O (20.0 mg, 0.1 mmol) in MeOH (5 mL). The color of the mixture changed to dark red. Then, the mixture was concentrated to ca. 2 mL to form dark red solids, which were collected by filtration. The crude products were recrystallized with acetone to give dark red crystals (S)-7 of 54.0 mg (84% yield).

X-ray crystallographic analysis of (S)-7.



A clear dark orange column-like specimen of C₄₀H₂₆CuN₂O₃, approximate dimensions 0.100 mm x 0.400 mm x 0.400 mm, was used for the X-ray crystallographic analysis. The X-ray intensity data were measured.

The integration of the data using a monoclinic unit cell yielded a total of 23913 reflections to a maximum θ angle of 25.06° (0.84 Å resolution), of which 11568 were independent (average redundancy 2.067, completeness = 99.4%, $R_{\text{int}} = 1.87\%$) and 10939 (94.56%) were greater than $2\sigma(F^2)$. The final cell constants of $a = 15.2618(6)$ Å, $b = 13.0327(5)$ Å, $c = 17.7452(8)$ Å, $\beta = 108.0781(12)^\circ$, volume = 3355.3(2) Å³, are based upon the refinement of the XYZ-centroids of reflections above 20 $\sigma(I)$. The calculated minimum and maximum

transmission coefficients (based on crystal size) are 0.7700 and 0.9340.

The final anisotropic full-matrix least-squares refinement on F^2 with 876 variables converged at $R1 = 5.77\%$, for the observed data and $wR2 = 18.26\%$ for all data. The goodness-of-fit was 1.507. The largest peak in the final difference electron density synthesis was $2.510 \text{ e}^-/\text{\AA}^3$ and the largest hole was $-0.539 \text{ e}^-/\text{\AA}^3$ with an RMS deviation of $0.129 \text{ e}^-/\text{\AA}^3$. On the basis of the final model, the calculated density was 1.279 g/cm^3 and $F(000)$, 1332 e^- .

Table 1. Sample and crystal data for Naganawa5420.

Identification code	Naganawa5420
Chemical formula	$\text{C}_{40}\text{H}_{26}\text{CuN}_2\text{O}_3$
Formula weight	646.17
Temperature	93(2) K
Wavelength	0.71073 \AA
Crystal size	0.100 x 0.400 x 0.400 mm
Crystal habit	clear dark orange column
Crystal system	monoclinic
Space group	P 1 21 1
Unit cell dimensions	$a = 15.2618(6) \text{ \AA}$ $\alpha = 90^\circ$ $b = 13.0327(5) \text{ \AA}$ $\beta = 108.0781(12)^\circ$ $c = 17.7452(8) \text{ \AA}$ $\gamma = 90^\circ$
Volume	$3355.3(2) \text{ \AA}^3$
Z	4
Density (calculated)	1.279 g/cm^3
Absorption coefficient	0.691 mm^{-1}
F(000)	1332

Table 2. Data collection and structure refinement for Naganawa5420.

Theta range for data collection	2.19 to 25.06°
Index ranges	$-18 \leq h \leq 17$, $-15 \leq k \leq 15$, $-20 \leq l \leq 20$
Reflections collected	23913

Independent reflections	11568 [R(int) = 0.0187]
Max. and min. transmission	0.9340 and 0.7700
Refinement method	Full-matrix least-squares on F ²
Refinement program	SHELXL-2013 (Sheldrick, 2013)
Function minimized	$\Sigma w(F_o^2 - F_c^2)^2$
Data / restraints / parameters	11568 / 1 / 876
Goodness-of-fit on F²	1.507
Δ/σ_{\max}	0.008
Final R indices	10939 data; I>2 σ (I) R1 = 0.0577, wR2 = 0.1798 all data R1 = 0.0603, wR2 = 0.1826
Weighting scheme	w=1/[$\sigma^2(F_o^2)+(0.1000P)^2$] where P=(F _o ² +2F _c ²)/3
Absolute structure parameter	0.0(0)
Largest diff. peak and hole	2.510 and -0.539 eÅ ⁻³
R.M.S. deviation from mean	0.129 eÅ ⁻³

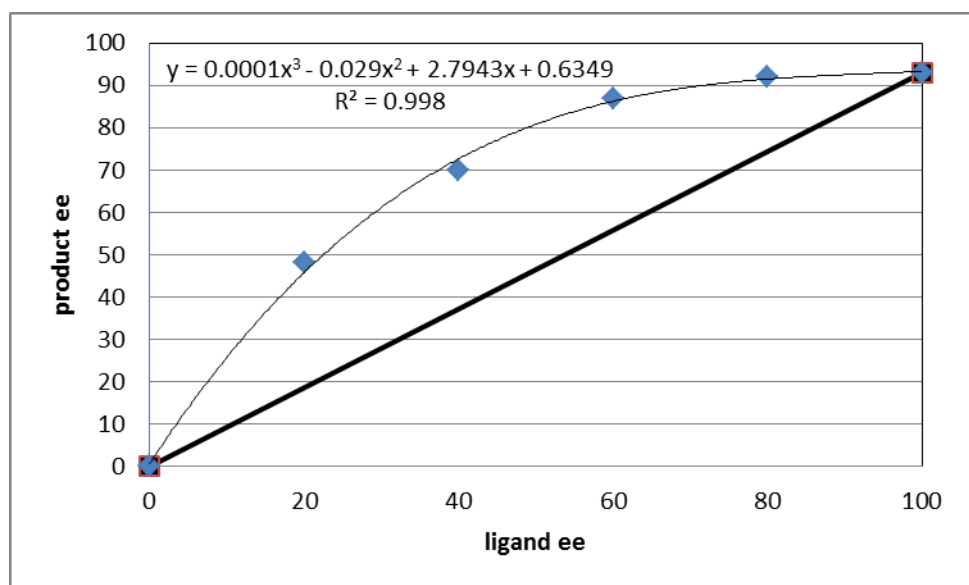
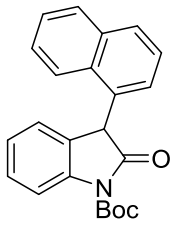


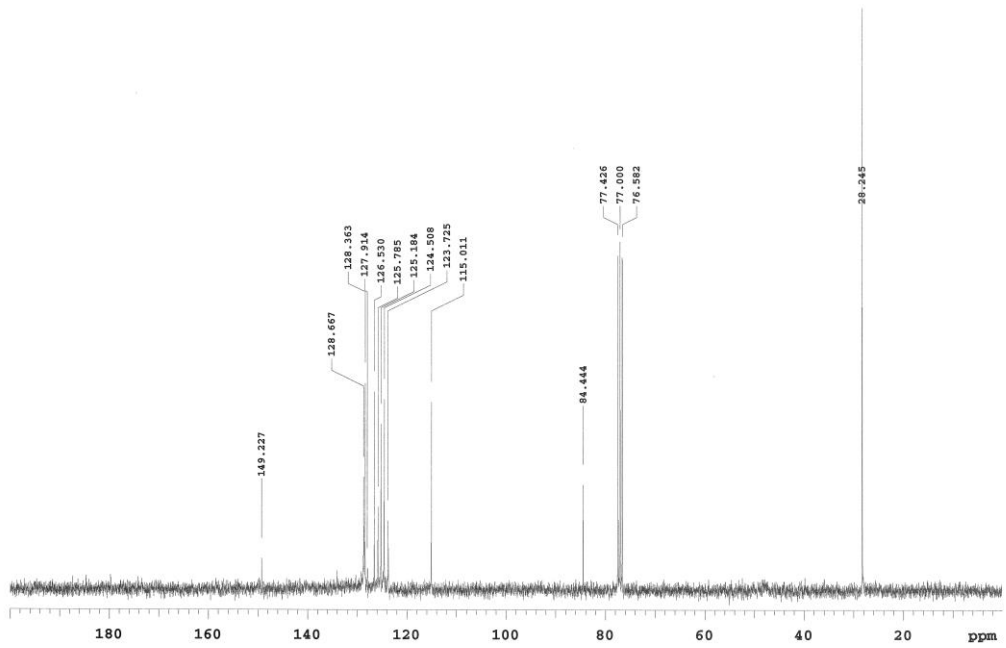
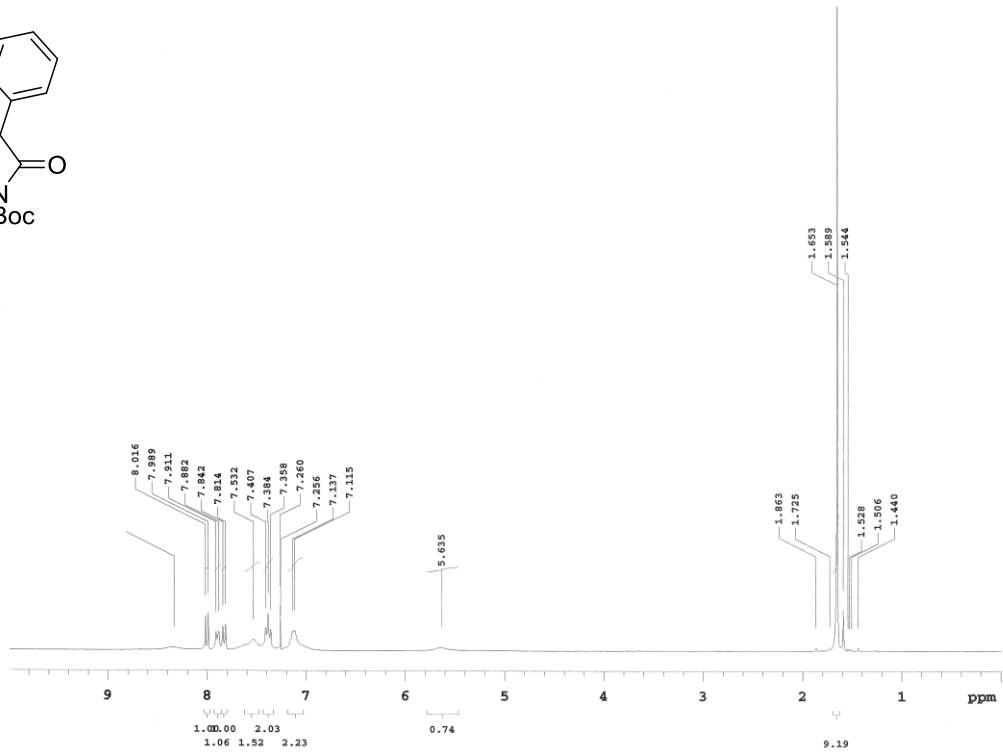
Figure S1. The relationship between ee of (*S*)-**2a** and ee of the product (*R*)-**1a**.
(refer to Table 3)

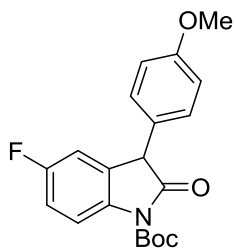
References.

- (S1) Y. Naganawa, T. Namba, T. Aoyama, K. Shoji, H. Nishiyama, H. *Chem. Commun.* **2014**, *50*, 13224.
- (S2) T. Ishimaru, N. Shibata, J. Nagai, S. Nakamura, T. Toru, S. Kanemasa, *J. Am. Chem. Soc.* **2006**, *128*, 16488.
- (S3) J. L. G. Ruano, J. Alemán, C. Fajardo, A. Parra, *Org. Lett.* **2005**, *7*, 5493.

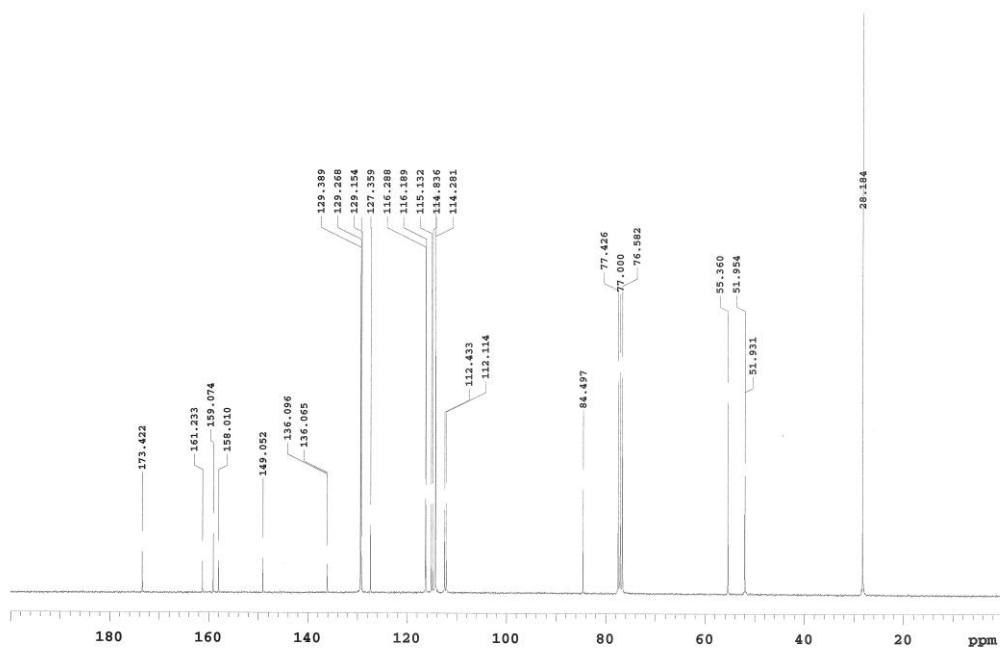
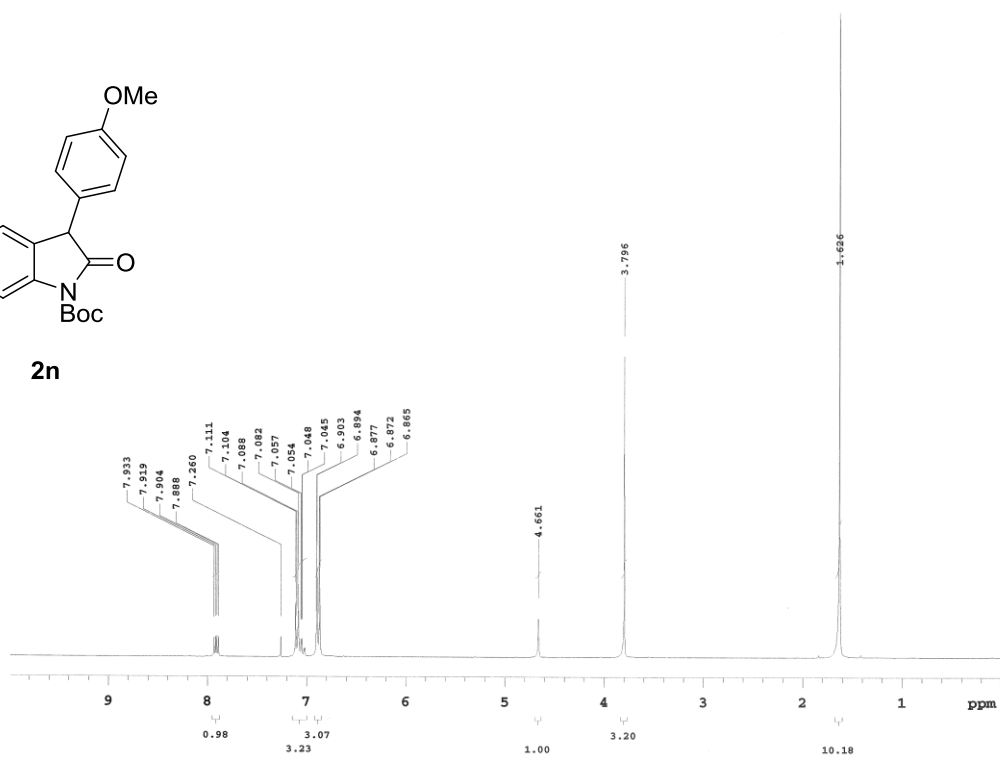


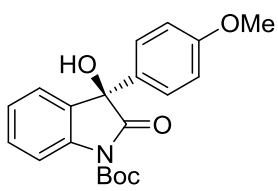
2g



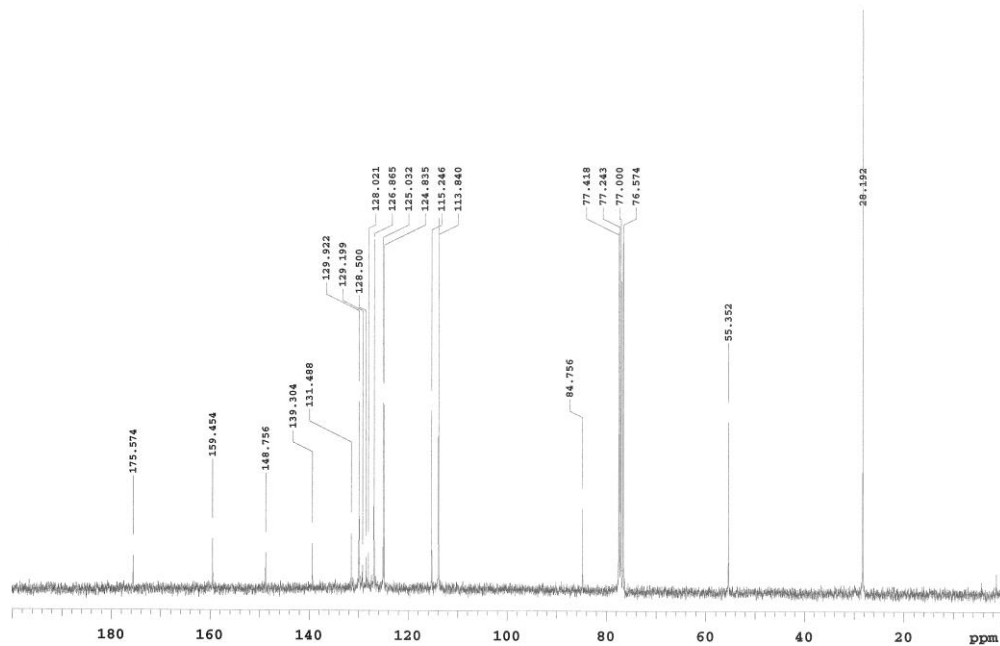
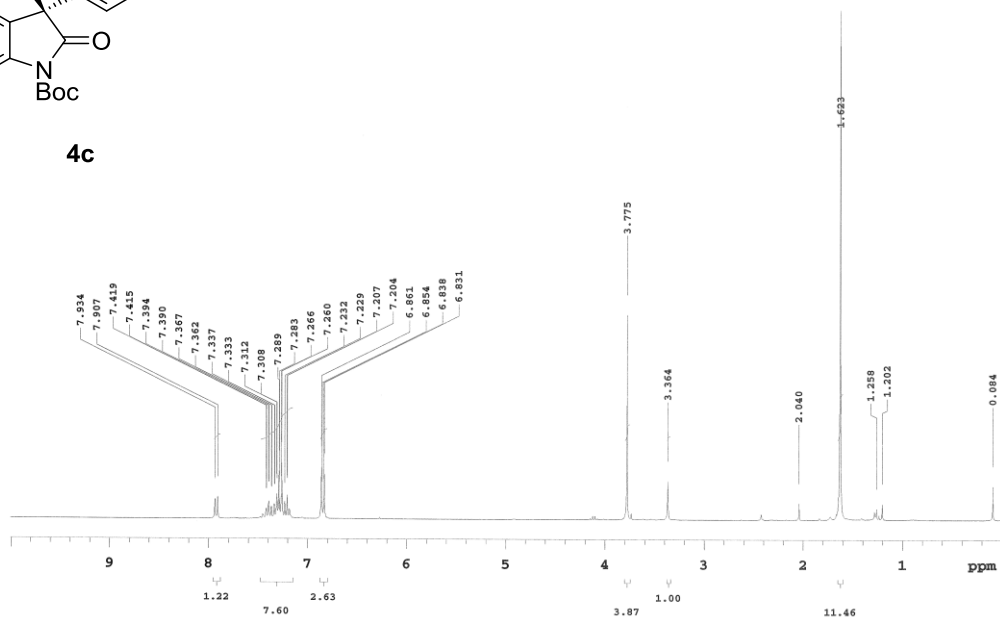


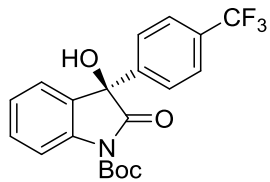
2n



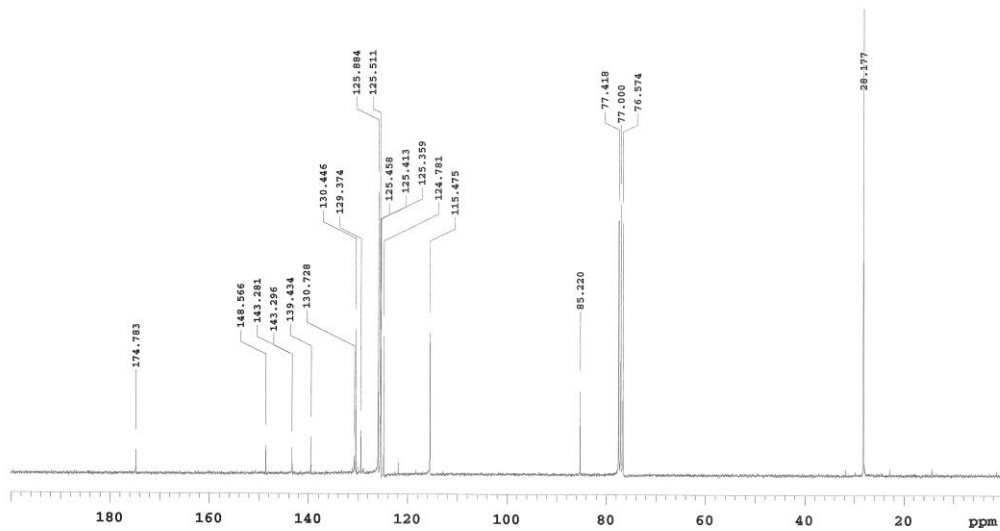
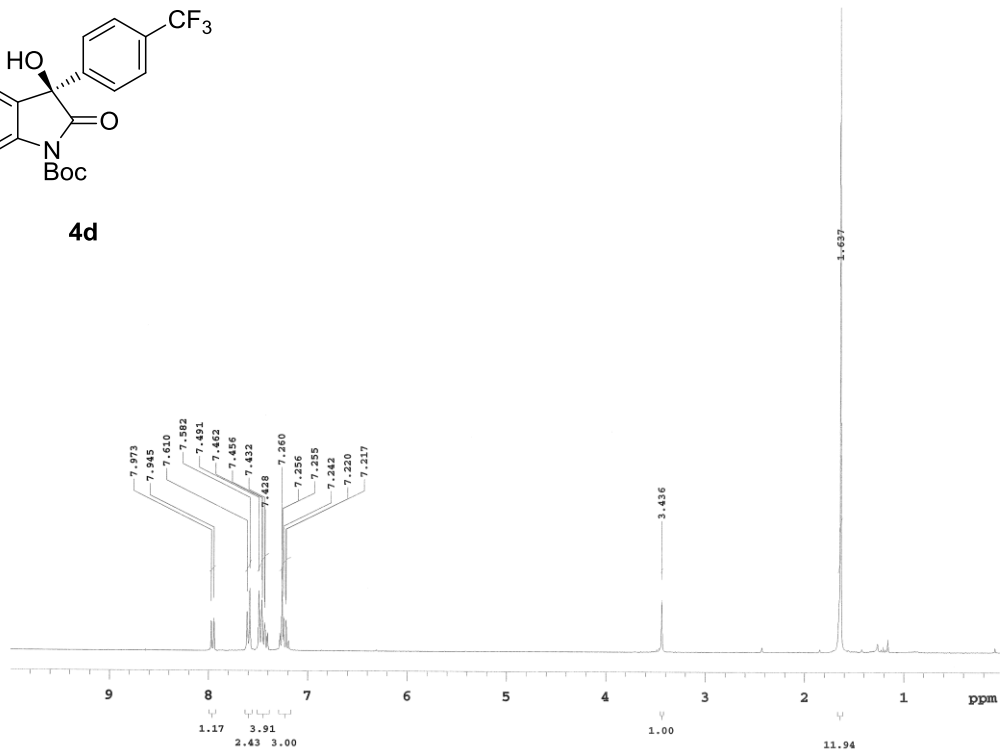


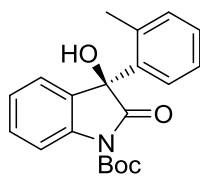
4c



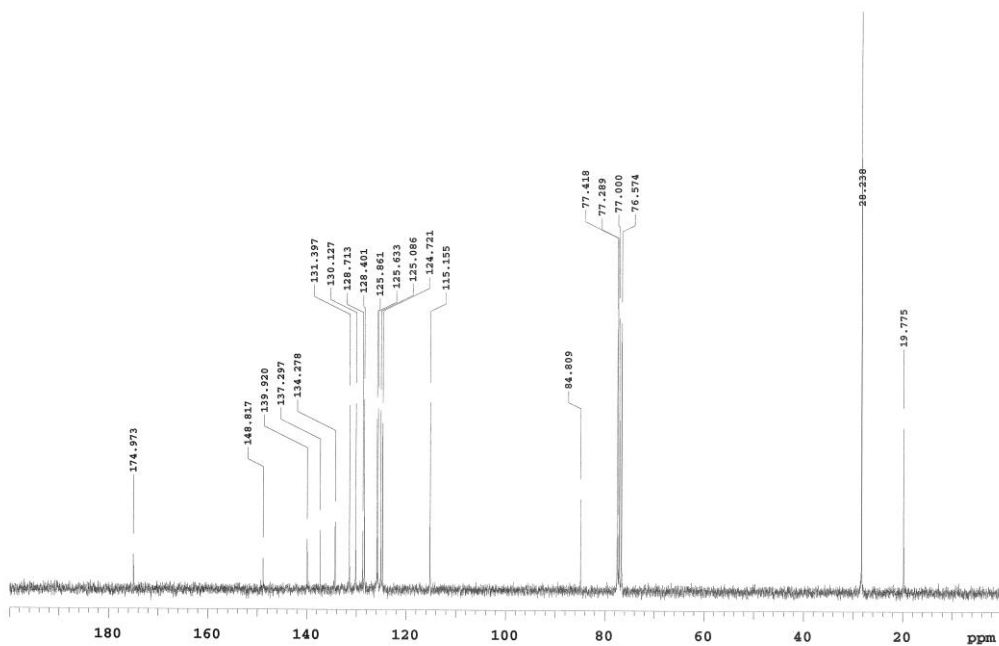
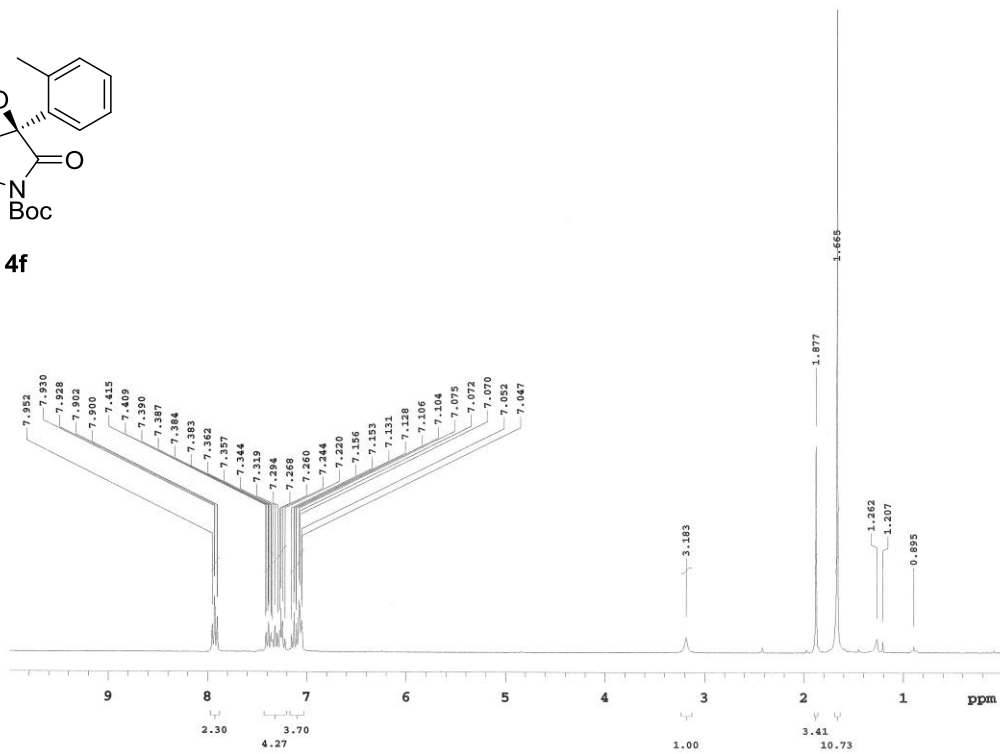


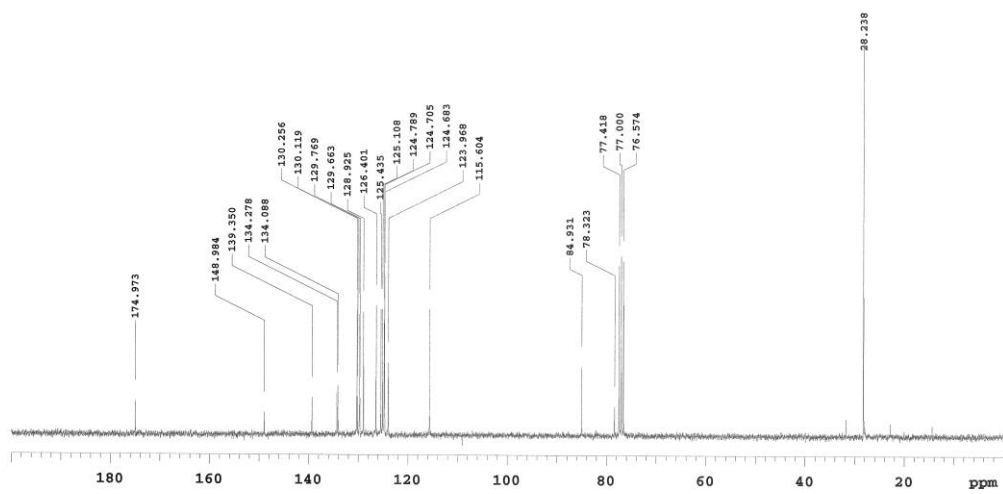
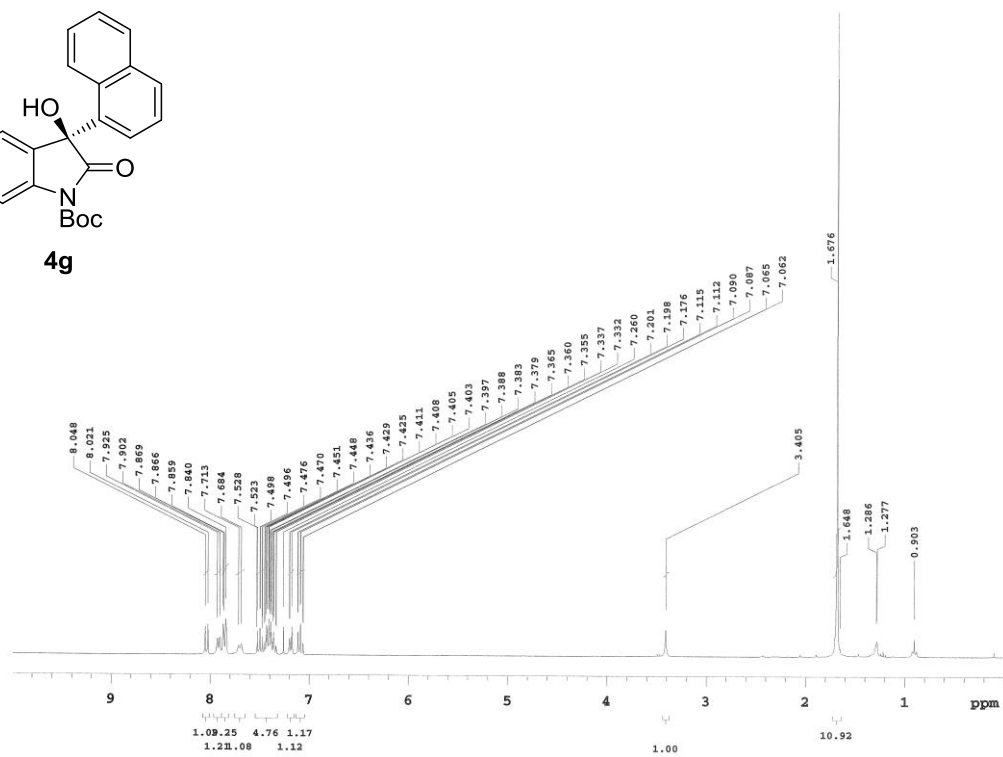
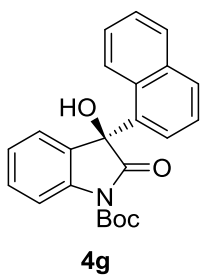
4d

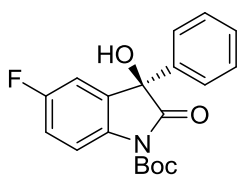




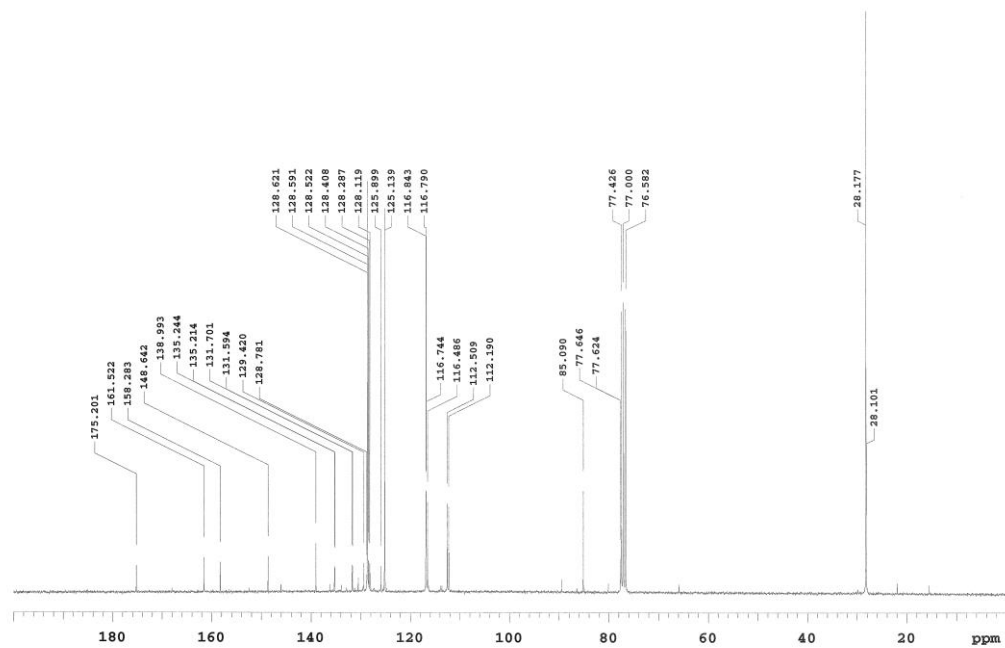
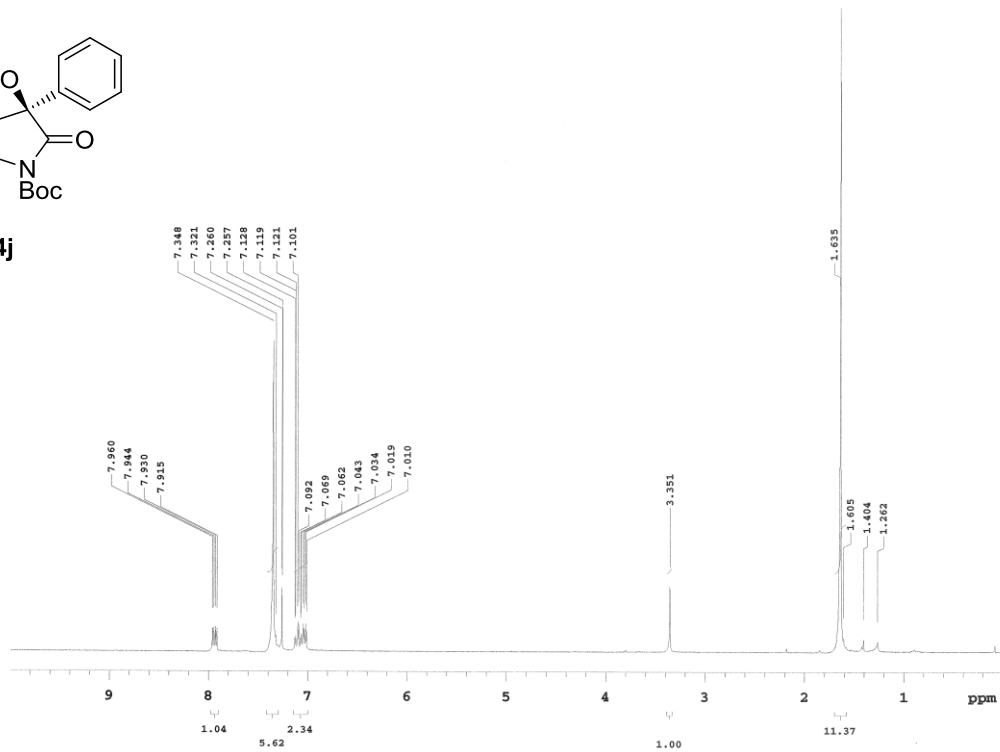
4f

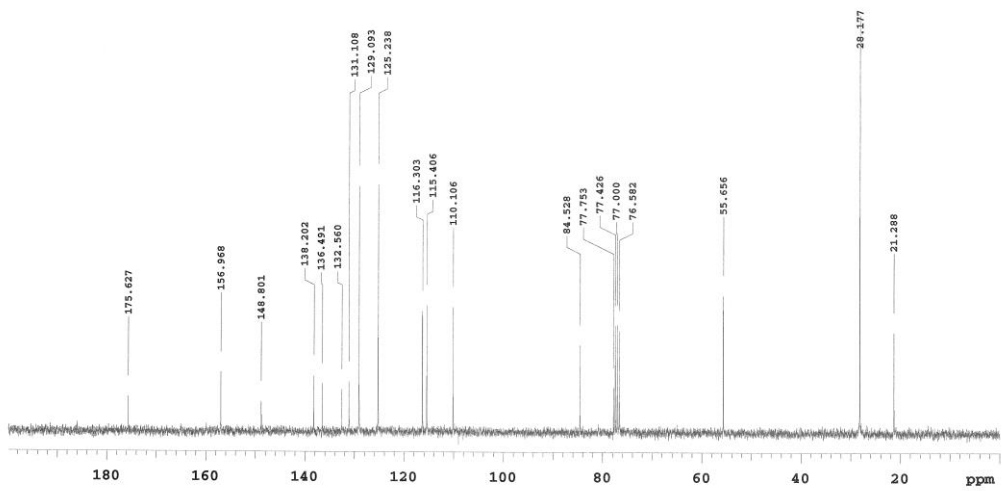
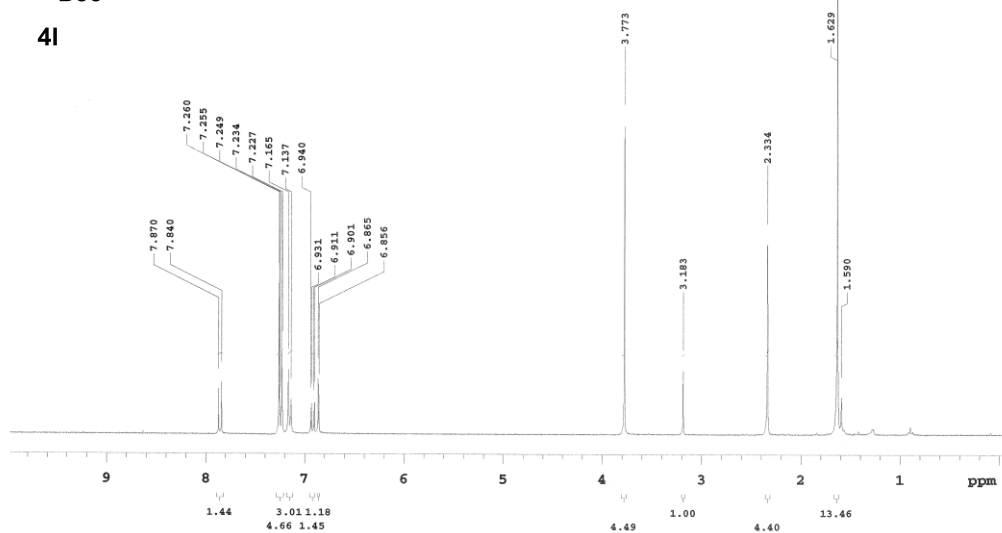
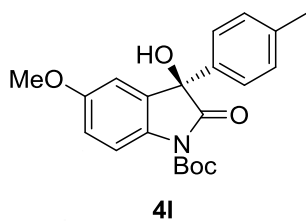


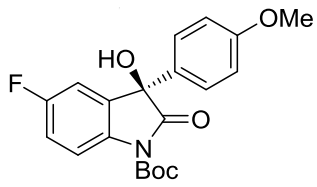




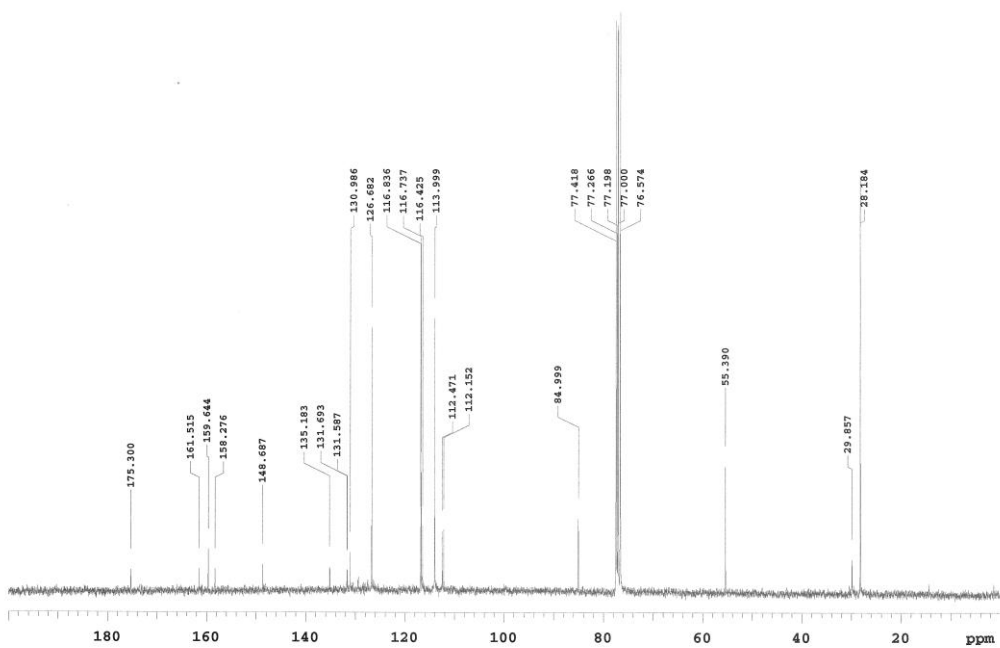
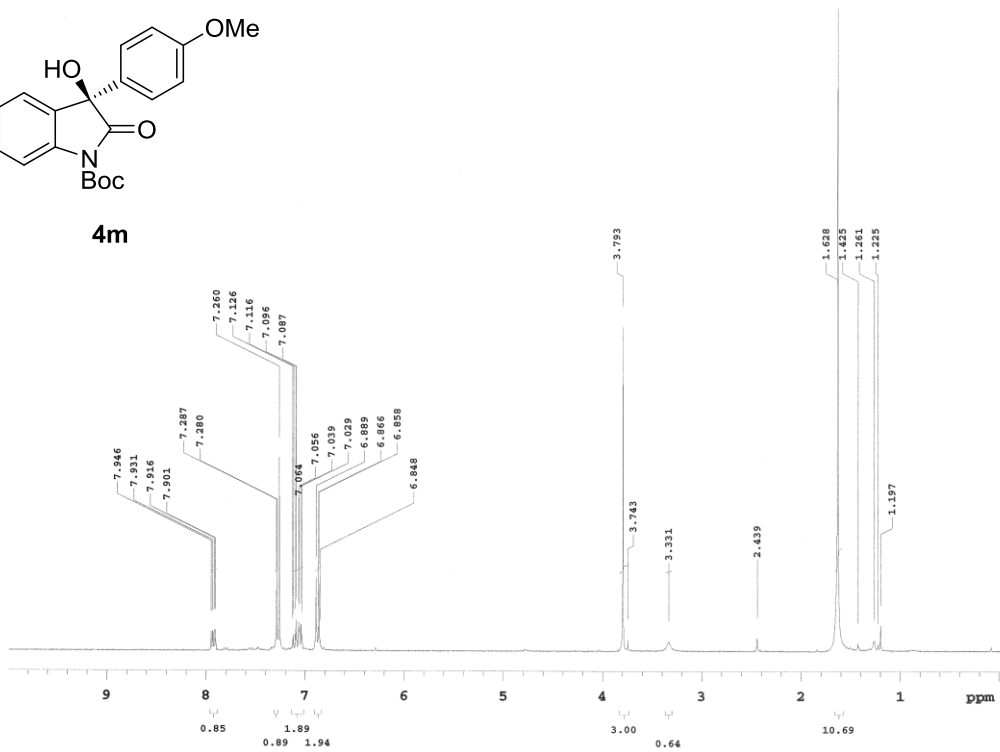
4j

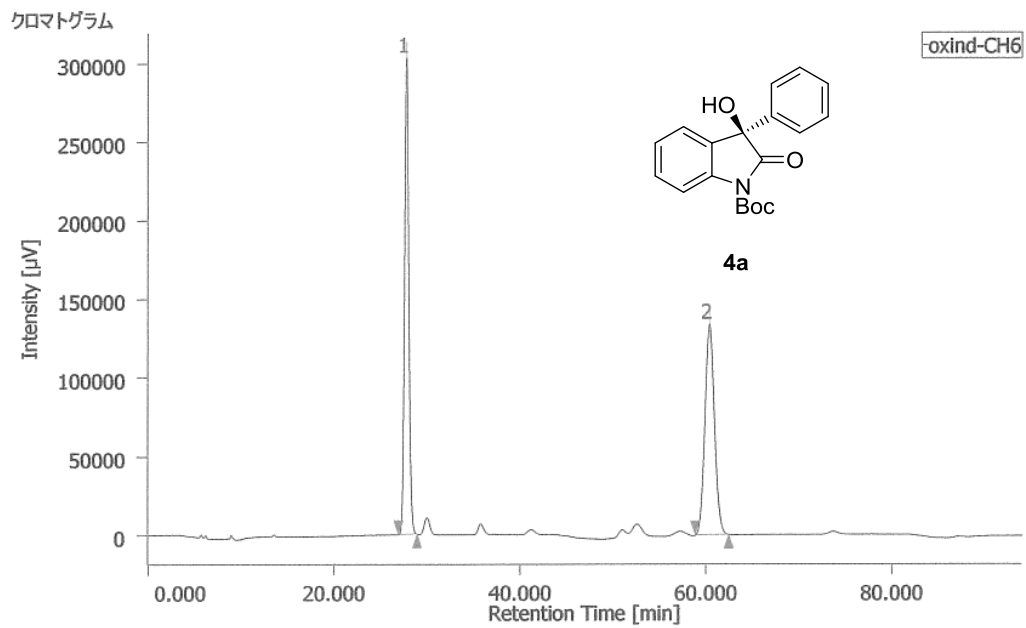






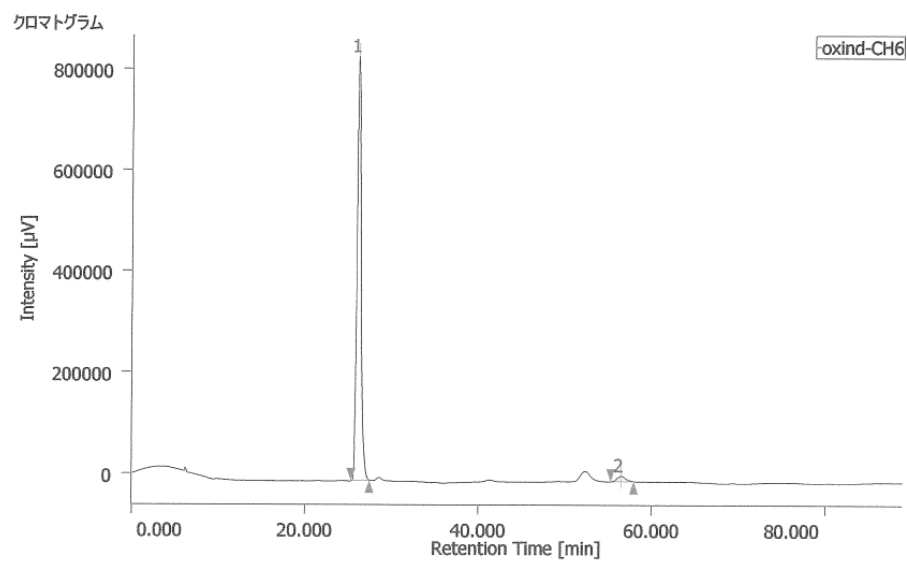
4m





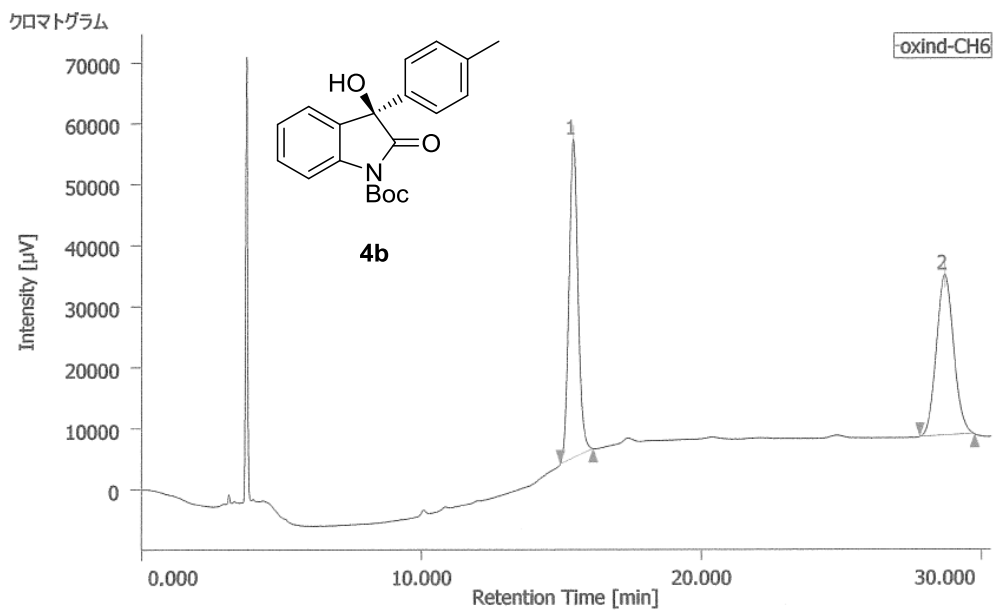
ピーク情報

#	tR [min]	Area [$\mu\text{V}\cdot\text{sec}$]	Height [μV]	Area%	Height%	NTP
1	27.810	9875771	303755	50.713	69.363	17193
2	60.390	9597944	134168	49.287	30.637	16524



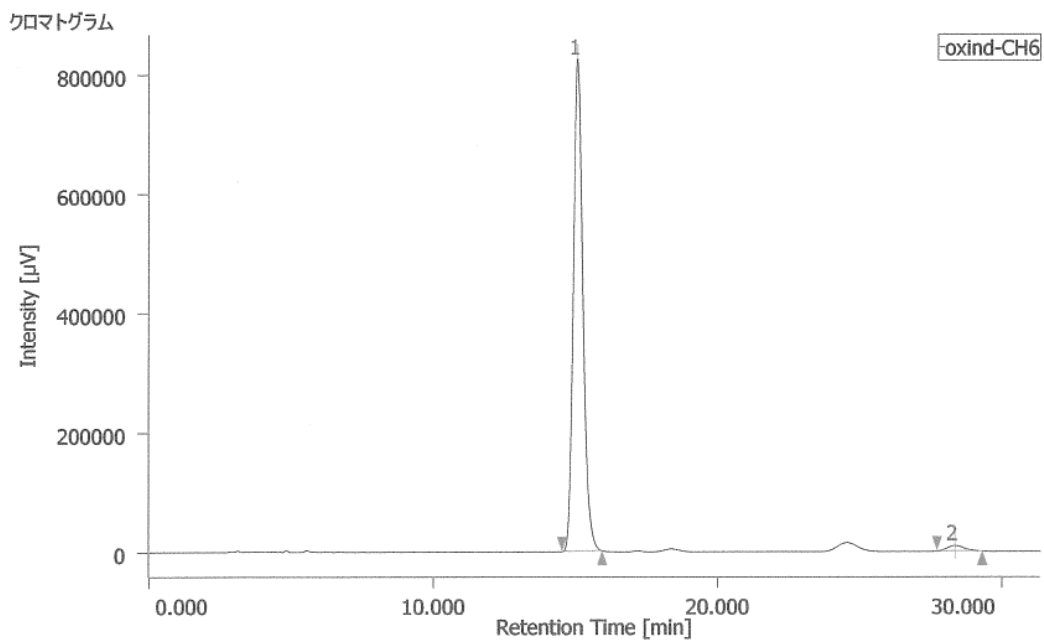
ピーク情報

#	tR [min]	Area [$\mu\text{V}\cdot\text{sec}$]	Height [μV]	Area%	Height%	NTP
1	26.097	28173821	838718	97.500	98.738	14989
2	56.455	722418	10722	2.500	1.262	15850



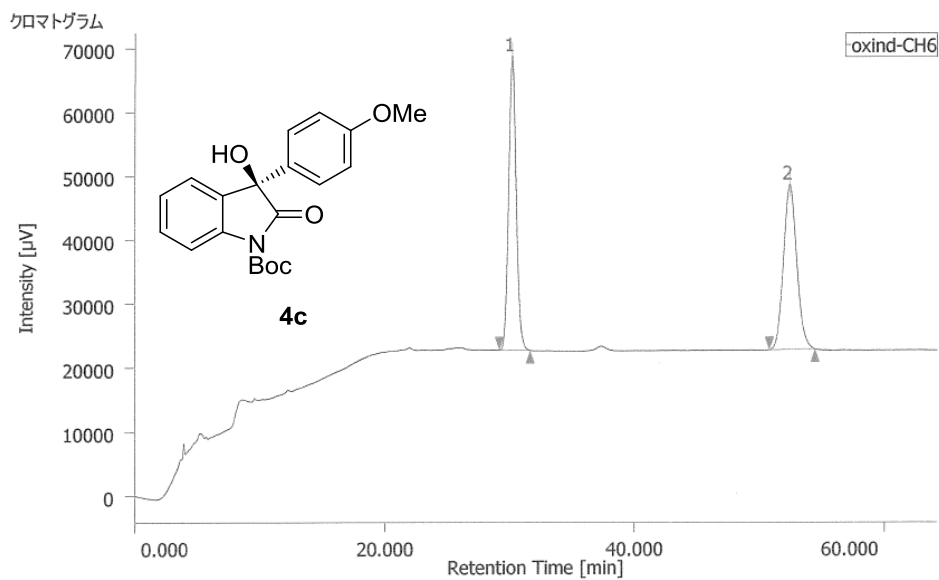
ピーク情報

#	tR [min]	Area [$\mu\text{V}\cdot\text{sec}$]	Height [μV]	Area%	Height%	NTP
1	15.408	1163028	52245	50.686	66.488	11425
2	28.668	1131566	26333	49.314	33.512	10317



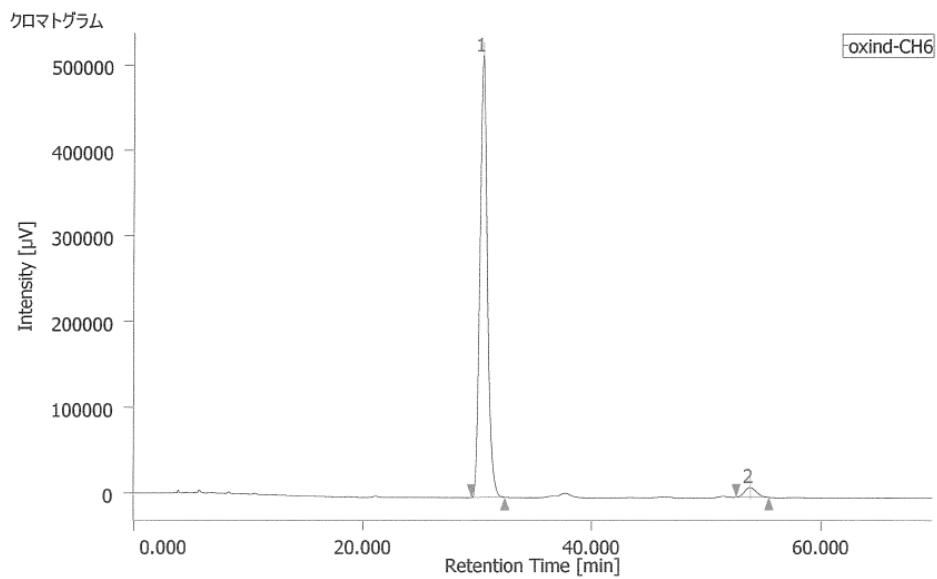
ピーク情報

#	tR [min]	Area [$\mu\text{V}\cdot\text{sec}$]	Height [μV]	Area%	Height%	NTP
1	15.067	19605027	824811	97.998	98.889	9700
2	28.328	400605	9270	2.002	1.111	9678



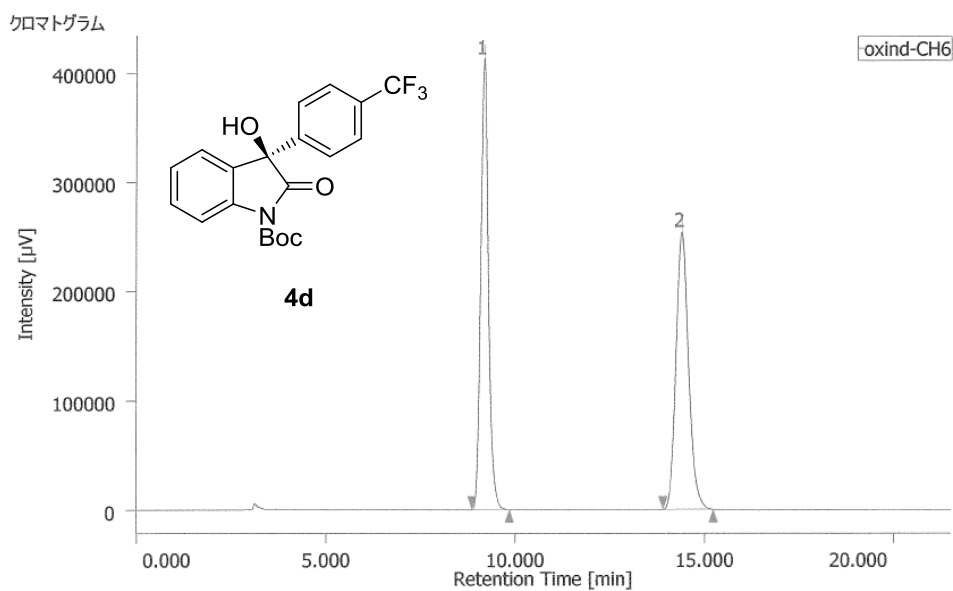
ピーク情報

#	tR [min]	Area [$\mu\text{V}\cdot\text{sec}$]	Height [μV]	Area%	Height%	NTP
1	30.173	1941992	46163	50.361	64.107	12254
2	52.418	1914148	25847	49.639	35.893	11783



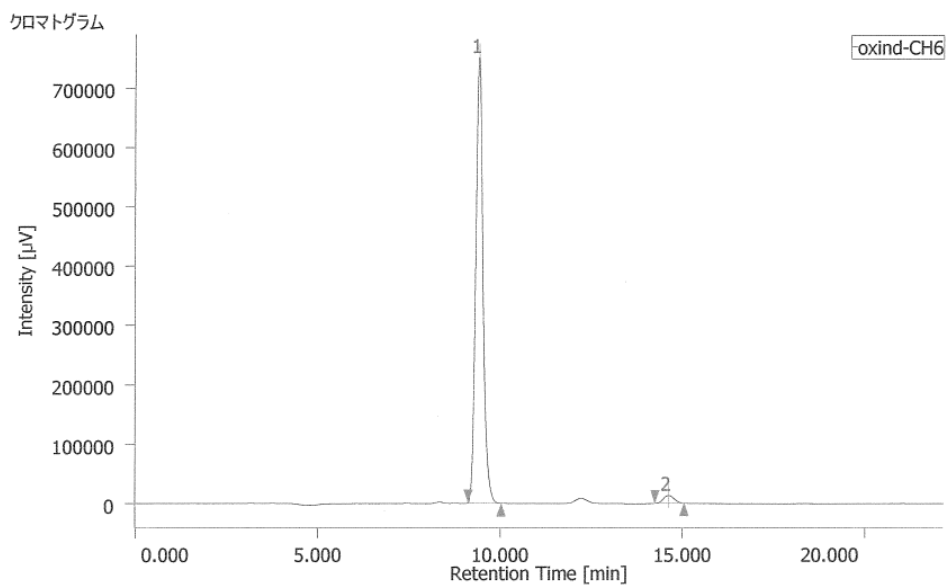
ピーク情報

#	tR [min]	Area [$\mu\text{V}\cdot\text{sec}$]	Height [μV]	Area%	Height%	NTP
1	30.463	23454450	516734	96.484	97.802	10968
2	53.845	854797	11611	3.516	2.198	11981



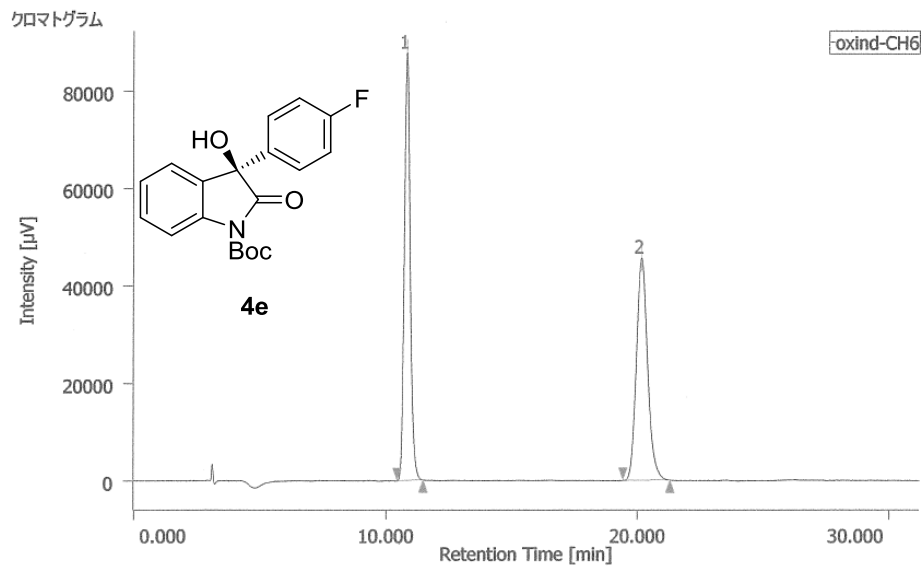
ピーク情報

#	tR [min]	Area [$\mu\text{V}\cdot\text{sec}$]	Height [μV]	Area%	Height%	NTP
1	9.175	5837213	413525	49.991	61.881	10363
2	14.395	5839272	254734	50.009	38.119	9523



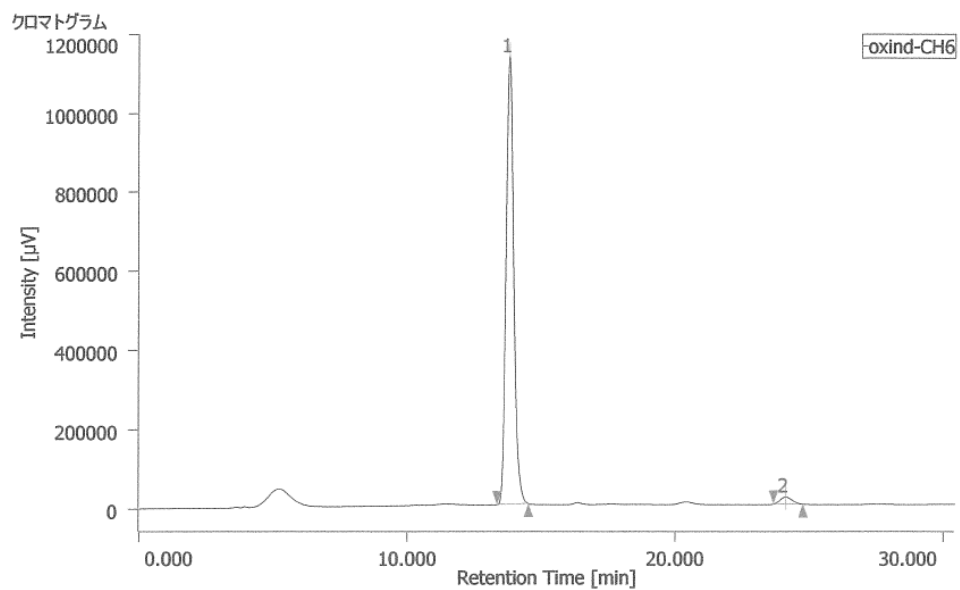
ピーク情報

#	tR [min]	Area [$\mu\text{V}\cdot\text{sec}$]	Height [μV]	Area%	Height%	NTP
1	9.407	10480863	752510	97.401	98.256	11092
2	14.617	279634	13353	2.599	1.744	10796



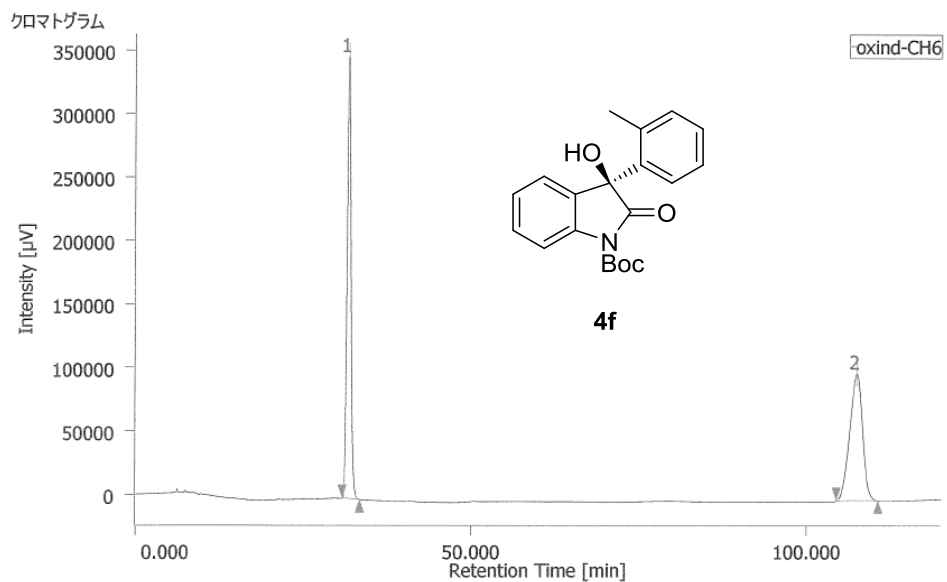
ピーク情報

#	tR [min]	Area [$\mu\text{V}\cdot\text{sec}$]	Height [μV]	Area%	Height%	NTP
1	10.840	1413957	87877	49.944	65.828	11142
2	20.155	1417153	45618	50.056	34.172	10241



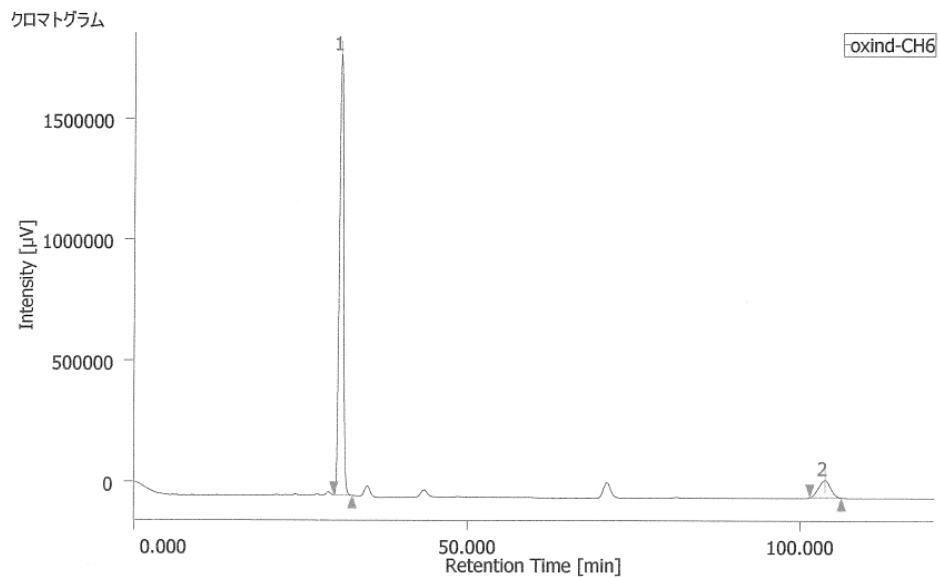
ピーク情報

#	tR [min]	Area [$\mu\text{V}\cdot\text{sec}$]	Height [μV]	Area%	Height%	NTP
1	13.798	22120005	1132308	97.530	98.407	12179
2	24.118	560306	18326	2.470	1.593	13495



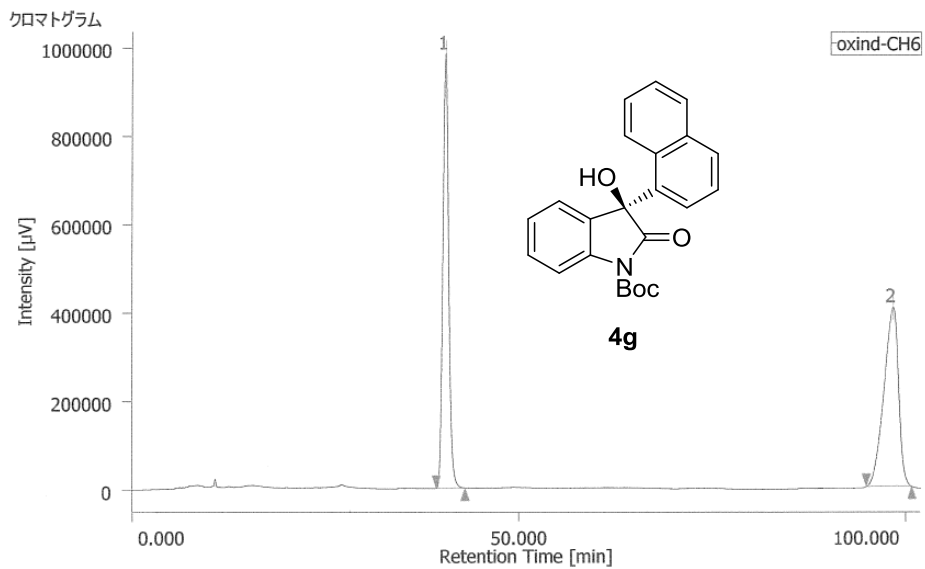
ピーク情報

#	tR [min]	Area [$\mu\text{V}\cdot\text{sec}$]	Height [μV]	Area%	Height%	NTP
1	31.777	13589797	348724	50.354	77.684	15910
2	107.450	13398614	100177	49.646	22.316	14843



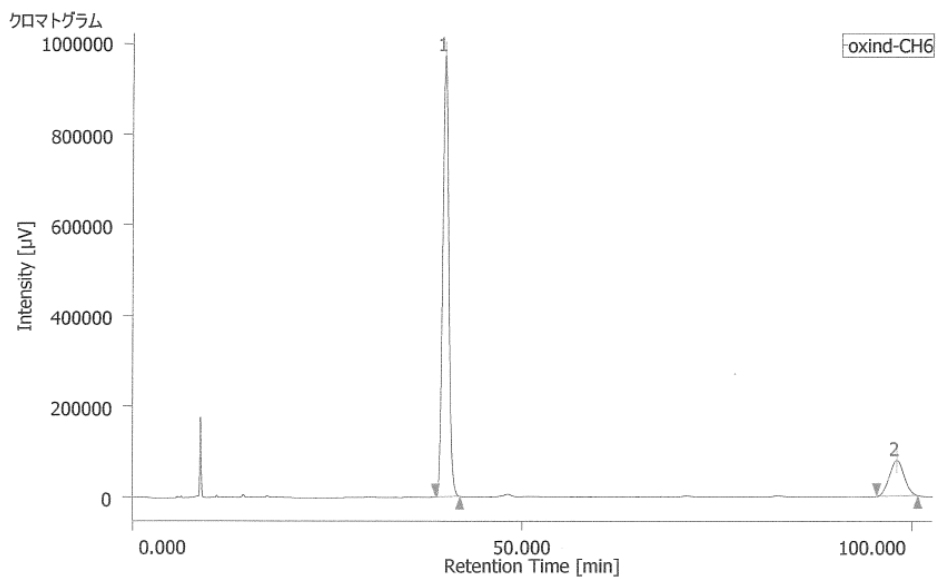
ピーク情報

#	tR [min]	Area [$\mu\text{V}\cdot\text{sec}$]	Height [μV]	Area%	Height%	NTP
1	31.028	80474784	1819777	90.048	96.202	11082
2	103.642	8893538	71845	9.952	3.798	15469



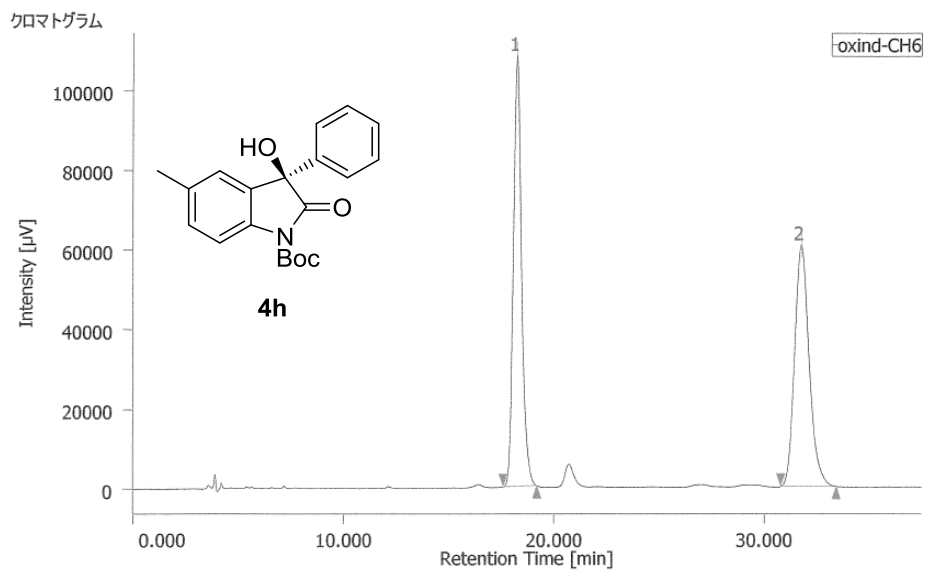
ピーク情報

#	tR [min]	Area [$\mu\text{V}\cdot\text{sec}$]	Height [μV]	Area%	Height%	NTP
1	40.450	52530848	984454	49.550	70.774	13645
2	98.313	53485254	406522	50.450	29.226	12650



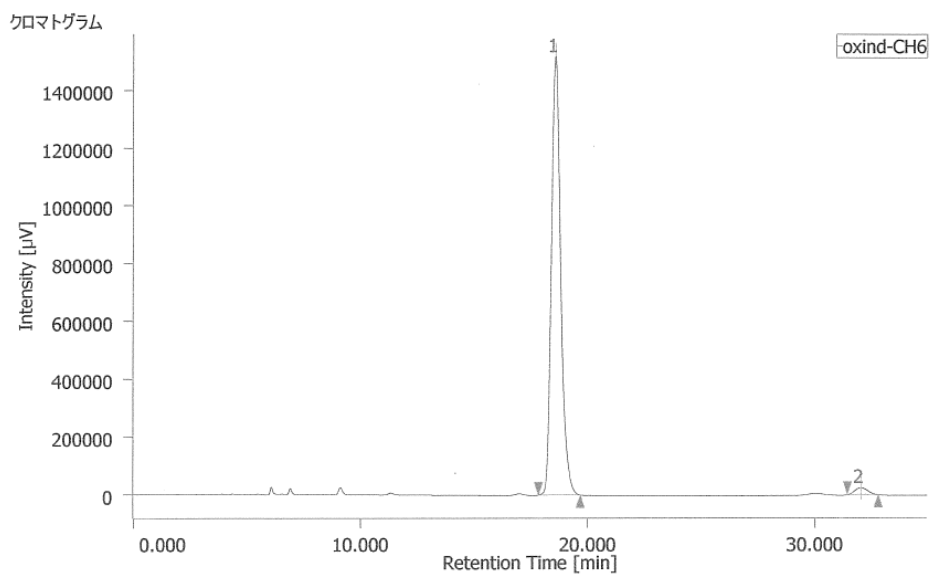
ピーク情報

#	tR [min]	Area [$\mu\text{V}\cdot\text{sec}$]	Height [μV]	Area%	Height%	NTP
1	40.052	51990823	973956	83.479	92.525	13278
2	98.017	10289149	78679	16.521	7.475	12621



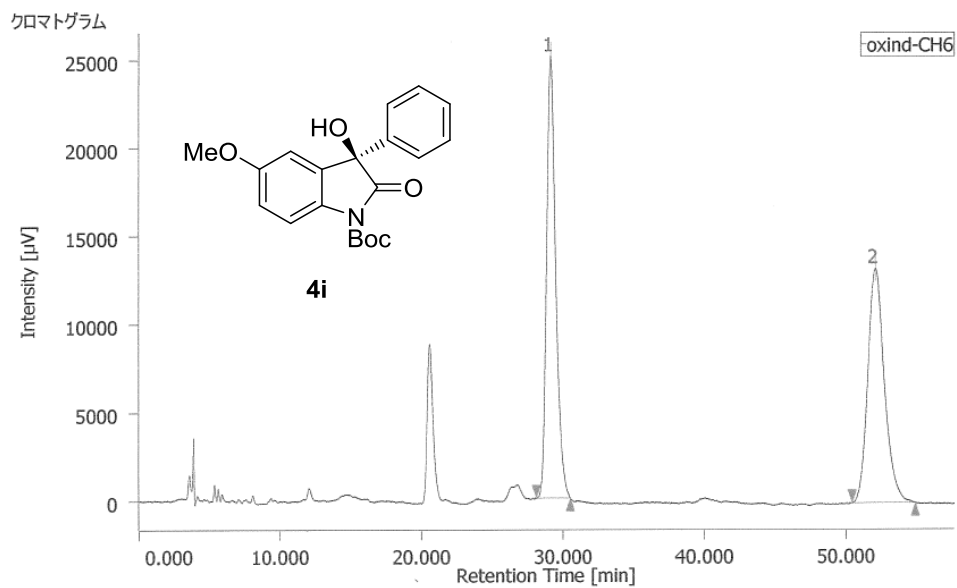
ピーク情報

#	tR [min]	Area [$\mu\text{V}\cdot\text{sec}$]	Height [μV]	Area%	Height%	NTP
1	18.237	2944007	108428	50.230	64.090	11166
2	31.725	2917042	60753	49.770	35.910	10637



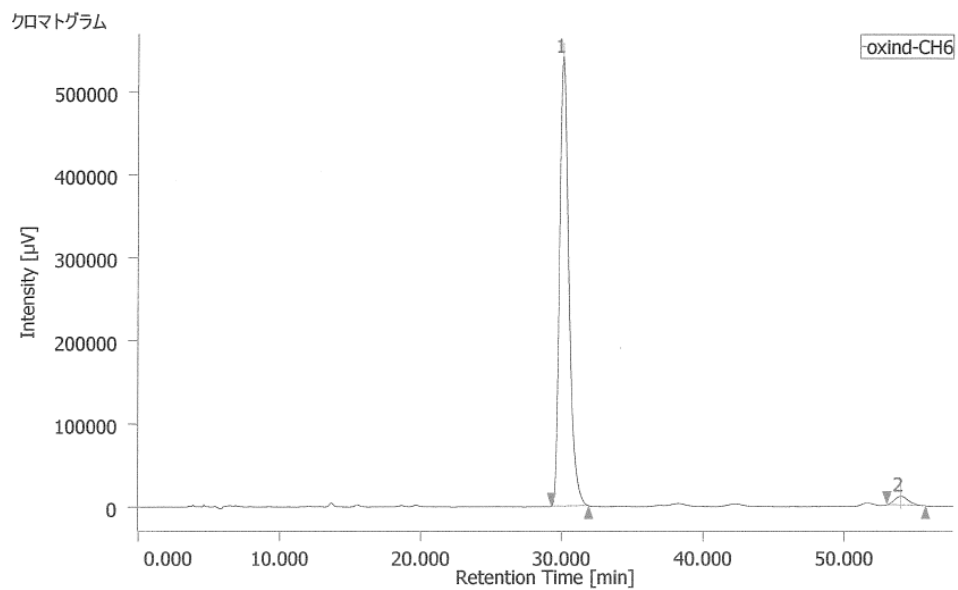
ピーク情報

#	tR [min]	Area [$\mu\text{V}\cdot\text{sec}$]	Height [μV]	Area%	Height%	NTP
1	18.568	43622131	1522324	97.808	98.426	10242
2	32.013	977792	24343	2.192	1.574	13510



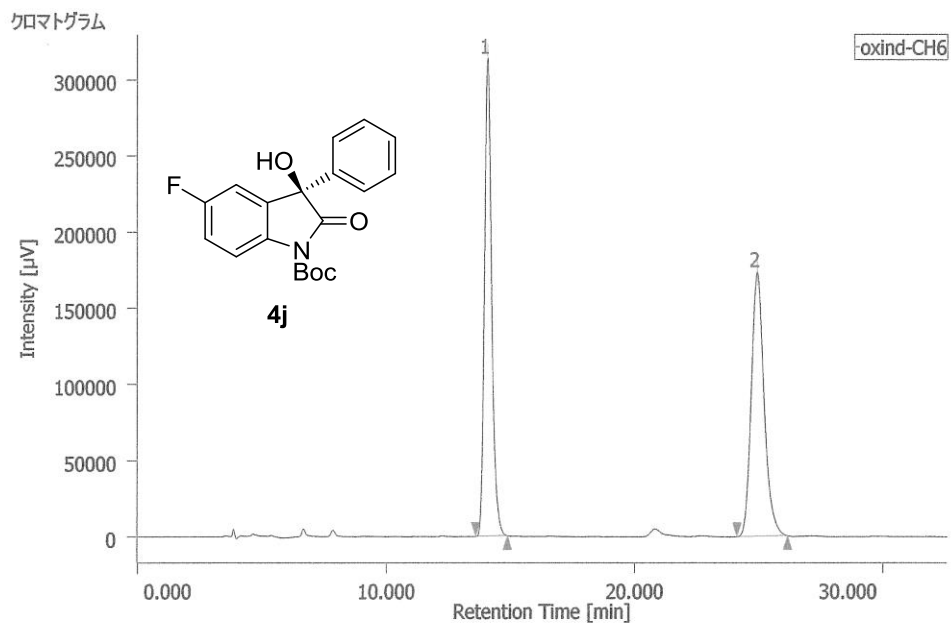
ピーク情報

#	tR [min]	Area [$\mu\text{V}\cdot\text{sec}$]	Height [μV]	Area%	Height%	NTP
1	29.102	1129783	25129	50.847	65.352	10329
2	52.042	1092130	13323	49.153	34.648	9890



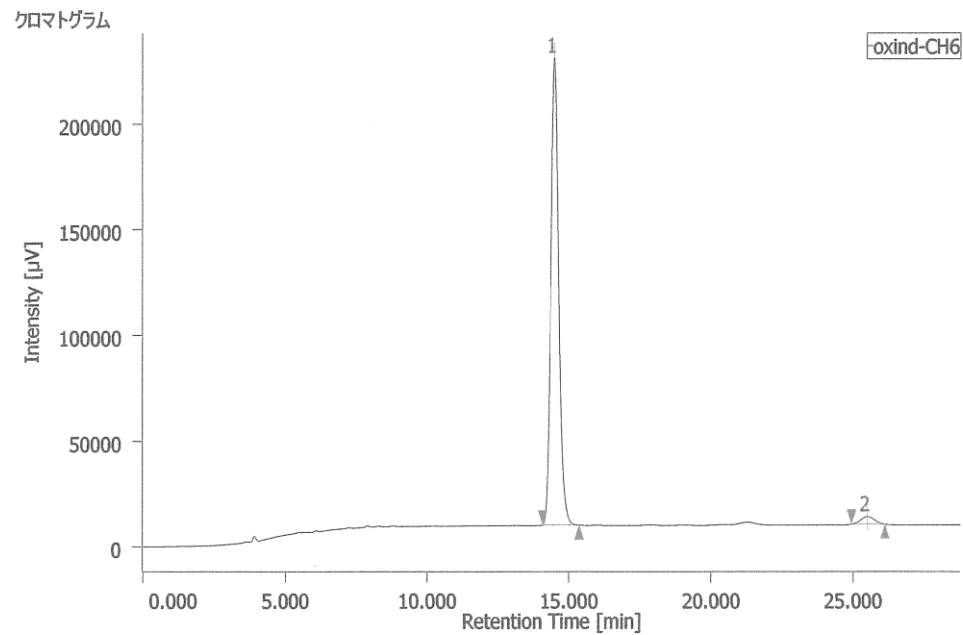
ピーク情報

#	tR [min]	Area [$\mu\text{V}\cdot\text{sec}$]	Height [μV]	Area%	Height%	NTP
1	30.085	24941729	541600	96.902	97.987	10532
2	53.967	797299	11129	3.098	2.013	12565



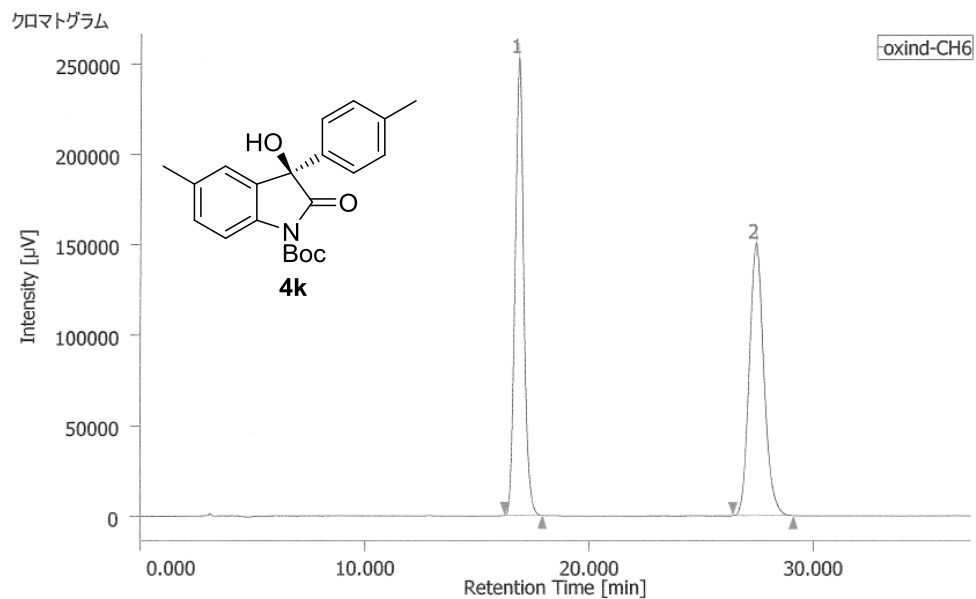
ピーク情報

#	tR [min]	Area [$\mu\text{V}\cdot\text{sec}$]	Height [μV]	Area%	Height%	NTP
1	14.080	6359835	313747	50.211	64.407	11998
2	24.903	6306464	173383	49.789	35.593	11471



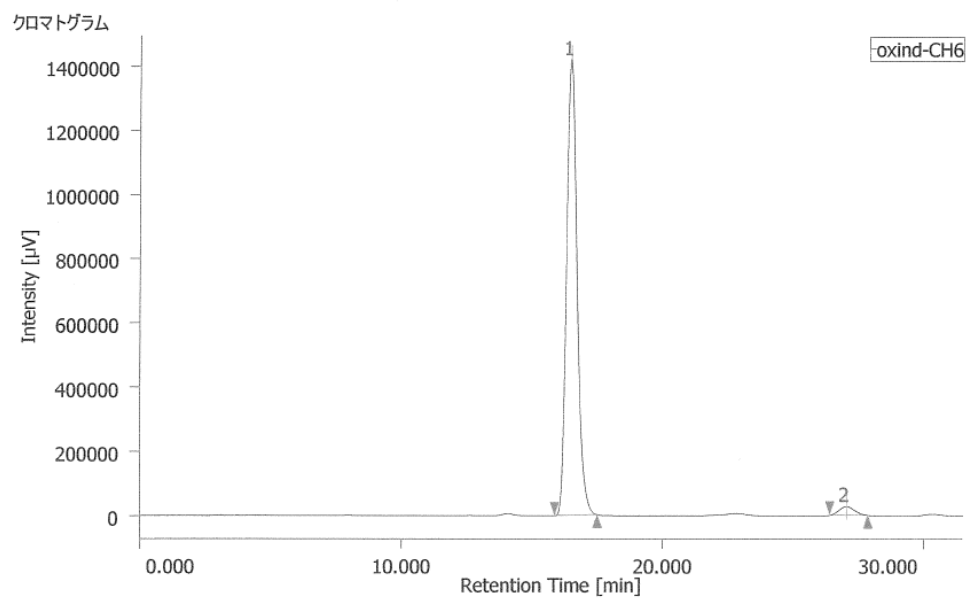
ピーク情報

#	tR [min]	Area [$\mu\text{V}\cdot\text{sec}$]	Height [μV]	Area%	Height%	NTP
1	14.485	4324876	221218	97.285	98.389	13245
2	25.493	120709	3623	2.715	1.611	12733



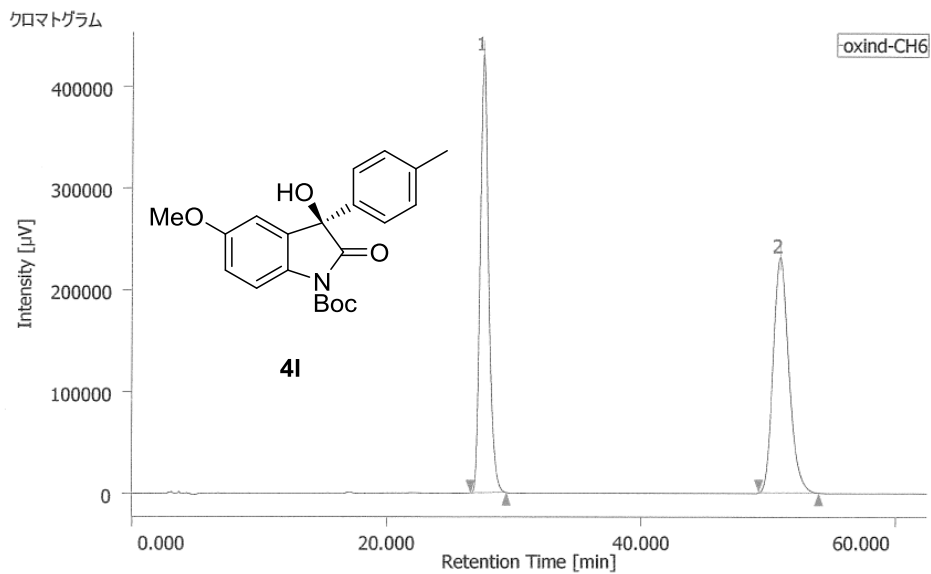
ピーク情報

#	tR [min]	Area [$\mu\text{V}\cdot\text{sec}$]	Height [μV]	Area%	Height%	NTP
1	16.833	6852715	253586	49.917	62.708	9399
2	27.400	6875404	150803	50.083	37.292	8658



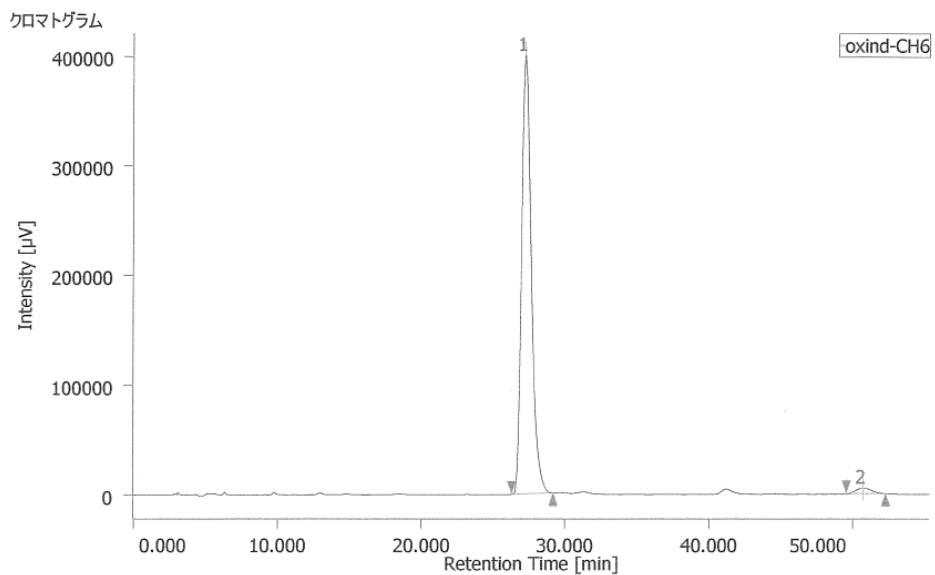
ピーク情報

#	tR [min]	Area [$\mu\text{V}\cdot\text{sec}$]	Height [μV]	Area%	Height%	NTP
1	16.465	39865810	1423247	97.256	98.096	8232
2	27.023	1124867	27624	2.744	1.904	9564



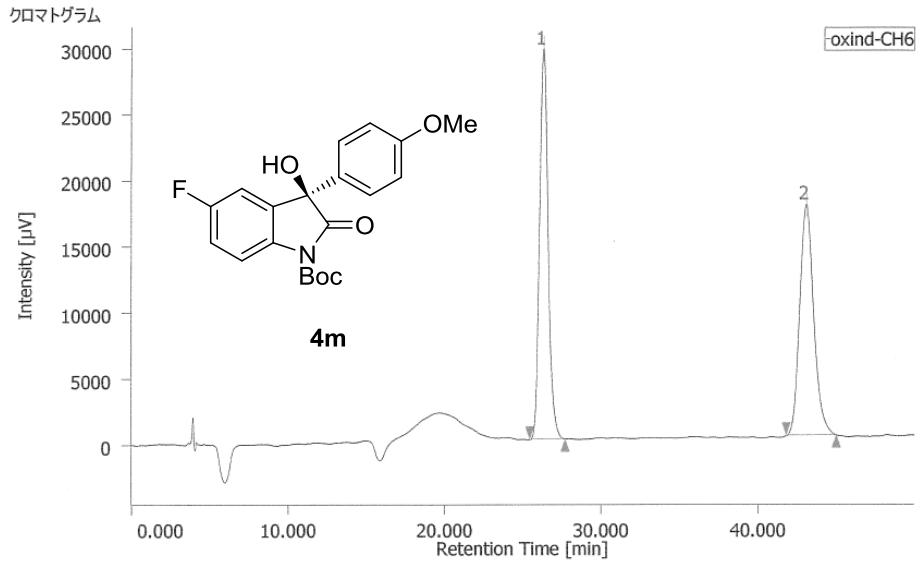
ピーク情報

#	tR [min]	Area [$\mu\text{V}\cdot\text{sec}$]	Height [μV]	Area%	Height%	NTP
1	27.548	20112283	431683	50.048	65.028	8454
2	50.863	20074002	232157	49.952	34.972	8276



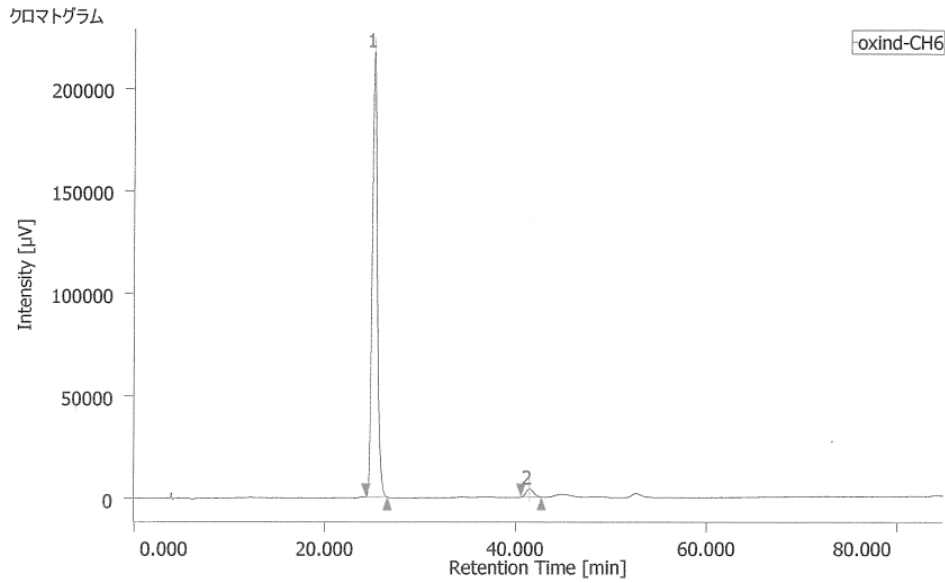
ピーク情報

#	tR [min]	Area [$\mu\text{V}\cdot\text{sec}$]	Height [μV]	Area%	Height%	NTP
1	27.230	18734285	400042	97.912	98.733	8252
2	50.698	399463	5133	2.088	1.267	9072



ピーク情報

#	tR [min]	Area [$\mu\text{V}\cdot\text{sec}$]	Height [μV]	Area%	Height%	NTP
1	26.297	1113458	29604	50.479	62.824	11933
2	43.088	1092320	17518	49.521	37.176	11467



ピーク情報

#	tR [min]	Area [$\mu\text{V}\cdot\text{sec}$]	Height [μV]	Area%	Height%	NTP
1	25.147	8052601	217439	97.241	98.207	11239
2	41.480	228490	3970	2.759	1.793	11569